A STUDY OF IN-MEDIUM NUCLEON-NUCLEON CROSS-SECTION

A Dissertation Submitted in Partial fulfillment of the requirements for the award of the degree

Of

Master of Philosophy
in Mathematics

By

SALMA PARVIN
Student No. 100009002F, Registration No. 0010242, Session October-2000
Department of Mathematics
Bangladesh University of Engineering and Technology
Dhaka-1000

Supervised

By

DR. NILUFAR FARHAT HOSSAIN
Professor
Department of Mathematics
BUET, Dhaka-1000

Bangladesh University of Engineering and Technology, Dhaka-1000

The Thesis Entitled

A STUDY OF IN-MEDIUM NUCLEON-NUCLEON CROSS-SECTION

Submitted by

SALMA PARVIN

Student No. 100009002F, Registration No. 0010242, Session October-2000, a fulltime student of M. Phil. (Mathematics) has been accepted as satisfactory in partial fulfillment

for the degree of

Master of Philosophy in Mathematics

On May 17, 2005.

Board of Examiners

1.	**Dr. Nilufar Farhat Hossain** Professor Department of Mathematics, BUET, Dhaka-1000.	Nilufarhat 17-05-05	Chairman (Supervisor)
2.	**Head** Department of Mathematics, BUET, Dhaka-1000.	Nilufarhat 17-05-05	Member (Ex-Officio)
3.	**Dr. Md. Mustafa Kamal Chowdhury** Professor Department of Mathematics BUET, Dhaka-1000.	M. Chowdhury 17.5.05	Member
4.	**Dr. Amal K Halder** Professor Department of Mathematics University of Dhaka, Dhaka-1000.	AHalder 17.05.05	Member (External)

Acknowledgement

All praises are due to Almighty Allah for enabling me to complete this dissertation successfully. This is a great pleasure to express my wholehearted gratitude and indebtedness to my reverend supervisor Dr. Nilufar Farhat Hossain, Professor, Department of Mathematics, Bangladesh University of Engineering and Technology. She has extended her full cooperation by offering constant advice, encouragement and proper guidance throughout the entire period of work and preparation of this thesis. Undoubtedly, it would be impossible to complete this work without her invaluable supervision.

I express my deep regards to my honorable teacher, Dr. Amal K Halder, Professor, Department of Mathematics, University of Dhaka for providing me help, advice and necessary guidance at every stage of my research work.

I also express my gratitude to my honorable teachers Professor Dr. Md. Zakerullah and Professor Dr. Md. Mustafa Kamal Chowdhury of the Department of Mathematics, Bangladesh University of Engineering and Technology for their invaluable guidance and helpful suggestions to complete this research work successfully. I also offer my best regards to all respected teachers of this Department for their affections, encouragement and kind cooperation.

I acknowledge the help, co-operation of all office staff of this Department.

Finally, I convey my regards to my beloved father and my husband who have initiated and encouraged me to accomplish this work properly.

Salma Parvin

SALMA PARVIN
Date: May 17, 2005

Candidate's Declaration

I hereby declare that the work which is being presented in the thesis entitled "A study of in-medium nucleon-nucleon cross-section" submitted in partial fulfillment of the requirement for the award of the degree of Master of Philosophy in Mathematics, in the Department of Mathematics, Bangladesh University of Engineering and Technology, Dhaka is an authentic record of my own work. I have not submitted the matter presented in this thesis for the award of any other degree in this or any other university.

Salma Parvin
(SALMA PARVIN)
Date: May 17, 2005

Abstract

It is the purpose of this thesis to provide a basis and a realistic starting point for systematic relativistic nuclear structure calculations in future. A family of realistic and quantitative nucleon-nucleon (NN) interaction potentials are constructed which are appropriate for application to relativistic NN scattering in the nuclear matter. The Brueckner *G*-Matrix theory in non-relativistic case is described and the theory is extended to relativistic Dirac-Brueckner formalism for the scattering of two nucleons in nuclear medium. The method of matrix inversion is also described for solving the Dirac-Brueckner *G*-matrix equation and hence finding the NN cross-sections in nuclear medium.

Finally, the dependence of NN cross-sections on the density of the nuclear medium is discussed by geometrical consideration of the Pauli blocking effect of the medium on free NN cross-sections. Some simple approximations show that for high energies the in-medium effect is less important and the free and in-medium NN cross-sections become approximately equal.

Contents

Introduction 1

Chapter 1: Nuclear force and nuclear matter 4

1.1 Meson theory and nuclear force

1.2 The idea of Massive-Particle Exchange

1.3 Empirical features of the nuclear force

1.4 Nuclear matter properties

Chapter 2: Boson fields and one-boson exchange potentials 18

2.1 Perturbation theory and Feynman rules

2.2 Various Boson fields and their couplings

2.3 One-boson exchange potentials and their contribution in NN interaction

Chapter 3: In-medium NN interaction and Dirac-Brueckner theory 36

3.1 Brueckner Theory and the *G*-matrix

3.2 The effective mass and the angle averaged Pauli operator

3.3 Thompson equation

3.4 The relativistic Dirac-Brueckner approach

Chapter 4: In-medium NN scattering cross-section and its density dependence 52

4.1 Matrix inversion method for solving Brueckner equation

4.2 Effective cross-sections for NN elastic scattering

4.3 The Golden rule for free NN cross-section

4.4 Geometrical consideration of the Pauli-blocking effect of the medium on NN cross-section

4.5 Density dependence of in-medium NN cross sections

Conclusion 74

References 76

Introduction

One of the fundamental goals of theoretical nuclear physics is to explain consistently the properties of nuclear matter, finite nuclei, and nuclear reactions (nucleon-nucleus as well as nucleus-nucleus collisions) with one realistic nucleon-nucleon (NN) interaction that has a solid theoretical basis and describes the two-body system accurately. First attempts towards this aim were based on the simplest model for the atomic nucleus: nucleons obeying the nonrelativistic Schrodinger equation interact through a two-body potential that fits the low-energy NN scattering data and the properties of the deuteron.

Historically, the first attempt was made by Heisenberg's student Euler who calculated the properties of nuclear matter in second-order perturbation theory assuming nucleons interacting via a two-body potential of Gaussian shape. When the singular nature of the nuclear potential at short distances ("hard core") was realized, it became apparent that conventional perturbation theory is inadequate. Special many-body methods had to be worked out. Brueckner, Levinson, and Mahmoud [1] initiated a method, which was further developed by Bethe [2].

In 1960s substantial advances in the physical understanding of Brueckner theory were made due to the work by Bethe and co-workers. Systematic calculations of the properties of nuclear matter applying Brueckner theory started in the late 1960s and continued through the 1970s. The work was done in the framework of Brueckner theory [1] by solving the Bethe-Goldstone equation, which yields an effective NN interaction in the medium [2-6]. The predictions by the nonrelativistic model for nuclear saturation with a variety of NN interactions show a systematic behavior: in an energy versus density plot the saturation points are located along a band, the so-called "Coester band" [7], which does not meet the empirical area.

Approaches discussed so far were based on the simplest model for the atomic nucleus: Nucleons obeying the non-relativistic Schrodinger equation interact through a two-body potential that fits low-energy NN scattering data and the properties of the deuteron. The failure of this model to explain nuclear saturation indicates that we may have to extend the model. One possible way is to include degrees of freedom other than the nucleon. The meson theory of the nuclear force suggests to consider, particularly, meson and isobar degrees of freedom. Characteristically, these degrees of freedom lead to medium effects on the nuclear force when inserted into the many-body problem as well as many-nucleon force contributions. In general, the medium effects are repulsive, whereas the many-nucleon force contributions are attractive. Thus there are large cancellations and the net result is very small. The density dependence of these effects/contributions is such that the saturation properties of nuclear matter are not improved [8]. One of the most important developments in the extension of nuclear many-body theory is the replacement of the non-relativistic Schrodinger equation with the relativistic Dirac equation to describe the single-particle motion in the medium [9].

In the 1970s a relativistic approach to nuclear structure was developed by Miller and Green [10]. They studied a Dirac-Hartree model for the ground state of nuclei, which was able to reproduce the binding energies, the root-mean-square radii, and the single-particle levels, particularly the spin-orbit splittings. Their potential consisted of a strong (attractive) scalar and (repulsive) vector component. At about the same time, Arnold, Clark, and Mercer applied a Dirac equation containing a scalar and a vector field to proton-nucleus scattering [11]. The most significant result of this Dirac phenomenology is the quantitative fit of spin observables, which are only poorly described by the Schrodinger equation.

Inspired by this success, a relativistic extension of Brueckner theory has been suggested by Shakin and co-workers [12], frequently called the Dirac-Brueckner approach. The advantage of a Brueckner theory is that the free NN interaction is used; thus there are no parameters in the force which are adjusted in the many-body problem The essential point of the Dirac-Brueckner approach is to use the Dirac equation for the single-particle motion in the nuclear matter. One of the main aspects to this problem is that one needs a realistic NN interaction potential which could be constructed in terms of meson-baryon interactions. Infact, the only quantitative NN interactions available up until now are based upon the idea of meson exchange; two well known example are the Paris potential and the Bonn potentials [8]. In most calculations a one-boson-exchange potentials are used for free NN interaction. The common feature of all Dirac-Brueckner results is that a (repulsive) relativistic many-body effect is obtained which is strongly density dependent such that the empirical nuclear matter saturation can be explained.

It is thus reasonable to apply and extend this approach to other domains of nuclear physics. An important application is the study of the properties of dense nuclear matter. These properties are important for particle physics, as well as nuclear physics. Experimentally, intermediate-energy heavy-ion reactions offer the unique opportunity to obtain a piece of dense nuclear matter in the laboratory. However, for the analysis of these reactions the properties of nuclear matter at high density are needed which can only be obtained from theoretical investigations [13]. In this sense, the theoretical investigation of the properties of dense nuclear matter, as well as the properties of hadrons in the dense medium [14], is of great importance.

In this work, we base our investigation on the Bonn meson-exchange model for the free NN interaction, the Dirac-Brueckner approach for the nucleon-nucleon (NN) scattering and the NN scattering cross-sections in the nuclear matter. In our work, we are concerned with elastic in-medium NN scattering which is the most important two body process in nucleus-nucleus collisions at incident energy below 300 MeV per nucleon. The work is designed in the following fastion:

In chapter one, we have a detail discussion on meson theory, nuclear force and nuclear structure properties (saturation density and energy). The Feynman rules for finding the amplitude for the scattering of two nucleons is also discussed. In chapter two, the Feynman rules are used to derive the one-boson exchange Bonn potentials for various boson fields.

In chapter three, we first discuss the Brueckner non-relativistic theory for the scattering of two nucleons in the nuclear matter. Secondly, we extend the theory to the relativistic case in the Dirac-Brueckner approach. Lastly, in chapter four, two methods for finding the in-medium cross-sections for the scattering of two nucleons in the nuclear matter along with the density dependence of the NN cross-sections are discussed in detail.

Chapter-1

Nuclear force and nuclear matter

Nowadays it has become customary in nuclear physics to denote by "tradition" the approach that considers nucleons and mesons as the relevant degrees of freedom It is the purpose of this chapter to review this traditional approach in the area of nuclear forces and nuclear structure. We look more closely into meson theory, to understand, in qualitative terms, what the meson exchange picture can predict for the NN system.

In section one, we review the history of meson theory and nuclear force. Yukawa's massive particle exchange, which gives the birth of particle physics, is discussed in section two. In section three, we give a brief review on some important empirical features of the nucleon force, which helps us to better asses the relevance of various meson exchange contributions. Finally, a discussion on the nuclear matter theory, which explains the empirical properties of nuclear structure is given in section four.

1.1 Meson theory and nuclear force:

The atomic nucleus was first discovered by Rutherford in the year of 1911. Thompson investigated the mass of nucleus and it was first assumed that nuclear models constitute of protons and electrons. In 1932 the neutron was discovered by Chadwick and this suggested that the neutron and proton were the fundamental constituents of nuclei.

But a question then arises, what holds the nucleus together? After all, the positively charged protons should repel one another violently, packed together as they are in such close proximity. Evidently there must be some other force, more powerful than the force of electrical repulsion that binds the protons and neutrons together. So it appeared compelling to assume the existence of a new force acting between neutrons and protons which binds the nucleus called the *strong force or nuclear force*, which is of very short range about the size of the nucleus itself. Heisenberg (1932) and Majorana (1933) introduced the concept of so called exchange forces, which could explain nuclear saturation.

The first significant theory of the strong force was proposed by Yukawa in 1934. Yukawa assumed that the proton and neutron are attracted to one another by some sort of field, just as the electron is attracted to the nucleus by an electric field. Yukawa's original theory was in classical field theory. Shortly after he reconsidered his proposal in quantized field theory. Since the short range of the force indicated that the mediator would be rather heavy; Yukawa suggested that the mass of its quantum should be 300 times that of the electron. Yukawa's particle came to be known as the *meson* (meaning middle weight) [In the same spirit the electron is called a lepton (light-weight), whereas the proton and neutron are baryons (heavy-weight)]. The massive character of the particle to be exchanged between the nuclear constituents would furnish the resulting force with a finite range desirable to account for nuclear saturation.

The well-known fundamental interactions in those days were the Coulomb interaction and the gravitational force, both having mathematically very simple form. Naturally, one expected something comparably simple for the nuclear potential, for example, just one Yukawa function: $\alpha \exp(-\mu r)/r$ (with r the distance between the two nucleons and $\mu = mc/h$, where m denotes the mass of the exchanged particle). However, even just phenomenologically, the nuclear force turns out to be much more complicated, mainly because of its dependence on the spins of the two interacting nucleons. In addition, field theory soon ran into fundamental mathematical difficulties.

In 1937 a *meson* was found in cosmic ray, the *muon*. It was interpreted as the particle predicted by Yukawa, particularly its mass ($\approx 106\,\text{MeV}$) appeared about right with regard to the range of the nuclear force and therefore, this discovery aroused considerable interest in Yukawa's idea. Kemmer felt inspired to suggest a rich variety of possible meson fields including pseudoscalar, axial-vector, and tensor, after Proca, in 1936 had already considered vector fields. Also a symmetric theory was proposed by Kemmer and Bhaba to account for the known hypothesis of charge independence. This suggestion was made in spite of the fact that experimentally only charged "mesons"(namely, μ^+ and μ^-)

were known. In lowest order, these cannot be exchanged between like nucleons and therefore seriously violate charge independence. It was also suggested that the two-meson exchange contribution could counterbalance this substantial inequality. The discovery of the quadrupole moment and the measurement of the magnetic moment of the deuteron by Rabi and co-workers in 1939 motivated immediately the development of more sophisticated models. Thus, it was realized that (isovector) vector fields create a tensor force giving rise to a quadrupole moment in the deuteron but with the wrong sign as compared to experiment. The problem was soon overcome by also including pseudoscalar fields. Pauli concluded from the fact that the pseudoscalar "symmetric" theory predicted the right sign for the quadrupole moment. This was the most correct theory, long before the pion was found and its spin and parity were determined. Also quite early it was recognized, that vector and scalar fields create a spin-orbit force. In 1947, Conversi, Pancini, and Piccioni showed that the muon does not interact strongly with nuclei and therefore, according to the notation introduced around 1960, it is not a meson: it is a *lepton*. That same year, a real meson with a mass of about 140 MeV, the *pion*, was found in a cosmic ray by Occhialini and collaborators.

Quite understandably, the new reality of a strongly interacting meson motivated vigorous theoretical efforts to describe the nuclear force, now, by the *pion only*. In 1951, Taketani, Nakamura, and Sasaki presented their suggestion to subdivide the nuclear force into three regions. They distinguish a *classical* (long-range, $r \geq 2$ fm; r denotes the distance between the centers of two nucleons), a dynamical (intermediate range, $1\,\text{fm} \leq r \leq 2\,\text{fm}$), and a phenomenological or core (short-range, $r \leq 1\,\text{fm}$) region. In the classical region the longest-range part of the potential, namely, the one-pion exchange (OPE) is dominant. In the intermediate range the two-pion exchange (TPE) is most important and finally, in the core region many different processes play a role. This classification has been utmost theoretical and of practical importance. It allows a step-by-step exploration of the two-nucleon interaction and permits a different derivation for different parts of the force.

In the decade under consideration, the one-pion exchange became experimentally well established as the long-range part of the nuclear force but the two-pion exchange evolves in an opposite way. It was difficult to evaluate and for a long time it did not even do well in correlating data. The many efforts of pion-theoretical potentials of the 1950s are usually divided into two groups; The Taketani-Machida-Onuma and the Brueckner-Watson types. In the former case an S matrix was evaluated directly from meson field theory, from which in turn a potential was derived. In contrast the latter method was based on an expansion in the particle number and derived a potential directly. Fortunately, there was also another line of research on the nuclear force during the 1950s; and it was the attempt to give a simple phenomenological description of the nuclear potential. The basis for the success of the phenomenological line for research on the nuclear force was the substantial progress in the NN scattering experiments of this period. From the properties of nuclear many-body system precise and detailed information regarding the force cannot be gained. Effective range theory had made clear that from low-energy data one cannot learn much more than what can be parameterized in terms of two numbers, the scattering length and the effective range. Therefore, it was obvious that high-energy data were required to obtain further insight into the nature of the nuclear force. Moreover, differential cross sections, even at high energy, are good only for a few rather basic and qualitative conclusions. Because of the important spin dependence of the NN interaction, data for many other observables are needed to specify the scattering amplitude.

The basic aim of a potential description of the two-nucleon interaction is twofold. One is to provide an economical summery of the data for comparison with potential-like results from theory. The other aim of a phenomenological potential is to serve as an input for nuclear calculations.

The most general form, a non-relativistic potential may assume, when taking also the spin degree of freedom of the nucleons into account, can be derived from invariance considerations. Restricting to at most linear dependence on the relative momentum of the two nucleons, p, it consists of *central, spin-spin, tensor* and *spin-orbit* terms. This phenomenological types of the potentials have been improved over the years. Other examples of the hard-core type are those constructed by Hamada and Johnston and by the Yale group. Both use the five-term form. These models employ a one-pion tail and therefore reproduce the deuteron properties accurately. In the mid 1960s R. V. Reid developed hard and soft-core potentials. One of his soft-core versions became the most applied potential in nuclear structure physics in the 1970s. Phenomenological potentials typically use 30-50 parameters.

Let us now return to the meson-theoretic work. The year 1960, was characterized by essentially two facts; the failure of the pion field-theoretic program, on the one hand, and a rich phenomenological experience with the nucleon-nucleon interaction (e.g. short-range repulsion and spin-orbit force), on the other. Not surprisingly, this led Breit and others to revive the old idea of vector-meson exchange, which predicts both features just mentioned. Further support came from the electromagnetic properties of nucleon. Nambu, Sakuri and Frazer and Fulco conjectured that vector bosons may play the dominant role in explaining the nuclear form factor. Their supposition was soon confirmed: In 1961, the ρ meson was discovered at Brookhaven in the $\pi^{-}p \rightarrow \pi\pi$ N reaction, and the ω meson was found at Berkeley in $\bar{p}p$ annihilation. Both are spin-1 bosons, the ρ being a 2π and the ω a 3π resonance, with masses around 770-780 MeV. The discovery of heavy mesons broke the deadlock situation in the meson theory of the nucleon-nucleon interaction. The first products of the new developments were the one-boson exchange (OBE) models. These models are based on the old Yukawa idea that the nuclear force is meson mediated.

There are also some very pragmatic reasons for the OBE model. First the evaluation of one-particle exchange processes is essentially straightforward, quite contrary to multiparticle exchanges, as we saw from the history of the 1950s. Second, within the OBE model the NN data can be described with very few parameters (of the order of 10, in contrast to phenomenological potentials, which typically need about 30-50). Since the OBE model parameters are meson-nucleon coupling constants and cutoffs, a physical meaning can be attributed to them, at least in principle.

Finally, the OBE concept was substantially improved by considering three-dimensional relativistic equations based upon the Bethe-Salpeter equation [15] and by working in momentum space to avoid the approximations necessary to obtain analytic r-space expressions. Work along this line was done by Schierholz, Thompson and others and the Bonn group.

Quite apart from the quantitative success of the OBEP in fitting the NN data, conceptually such models cannot be accepted as a comprehensive theory, as it is hard to believe that the uncorrelated multi-particle exchange should be totally negligible. The longest-range component of such exchanges, and therefore the most important of that kind, is the two-pion exchange (TPE). How to take the TPE more accurately or even completely into account was the other main topic of the 1960s. Naturally the new goal was to include all correlated and uncorrelated multi-particle exchanges, particularly for the case of two pions. In principle, there are two conceptually rather different ways to actually calculate these contributions: by field theory and by dispersion relations.

The principal framework of dispersion relation is based on three fundamental assumptions: causality, unitarity and crossing symmetry. From the first the analyticity of the reaction amplitude is concluded. The third allows one to relate processes that differ from each other only by the interchange of some incoming and outgoing particles of the reaction. Owing to analyticity, one particle exchange appears as a pole in the scattering amplitude. This fact can be exploited to extract empirical information about meson masses and particularly, meson-nucleon coupling constants. In the 1960's Amati, Leader and Vitale started work along this line, with which many groups soon got involved. The results showed that, for the intermediate range, a relativistic nuclear potential can be derived using dispersion relations and empirical information from πN and $\pi\pi$ scattering as input. Yet, these effects were still far from constructing a full quantitative nuclear potential.

In the course of the 1960s, the experimental program of the measurement of NN elastic scattering observables was pursued extensively by many accelerators throughout the world. As a result, by the end of the decade, the Livermore group could come up with a phase-shift analysis of NN scattering upto 425 MeV lab energy of high quality. This provided an important presupposition of the theoretical work of 1970s, which provides an absolutely quantitative nuclear force that is based on meson theory as much as possible. The work proceeded along the two lines discussed earlier: dispersion theory and field theory. Both approaches finally produced a very quantitative model. Most of this work was done in two Central European capitals; Paris and Bonn.

Let us first summarize the dispersion theoretic efforts. In continuation of the work of Chemtob *et al.*, the Stony Brook Group constructed a potential in which the dispersion theoretic result for the 2π exchange was complemented by one-π and one-ω exchange. For short distances the potential was regularized by the eikonal form factor derived by Woloshyn and Jackson. The fit to the NN scattering phase shifts was semi-quantitative. At about the same time, the Paris group produced a potential based on rather similar theoretical input. In the Paris case, the short-range part of the NN interaction was treated by an energy-dependent repulsive square-shaped cutoff. For the 2π exchange contribution to the nuclear potential both groups achieved even quantitative agreement. Further refinements and a convenient representation of the potential was left to the Paris group. Their final version, published in 1980, is parameterized in terms of static Yukawa functions of multiples of the pion mass [16].

Finally, let us turn to the field-theoretical attempts. After a decade of prevailing abstinence, the field-theoretical approach was revived by the work of Lomon and Partovi [17]. They evaluated the 2π exchange Fynmann diagrams with nucleons in the framework of the relativistic three-dimensional reduction of the Bethe-Salpeter equation proposed by Blankenbecler and Sugar [18]. It is a nonstatic approach to the 2π exchange. The old ambiguity of how to construct and subtract the iterated one-pion exchange when defining a potential was absent in this work. However, the models discussed so far left out contributions that are of substantial importance, like meson-nucleon resonances in intermediate states as well as three-pion and four-pion exchanges. In the mid 1970s the Bonn group started a program directed toward the evaluation of multipion exchange diagrams including nucleon resonances. This comprehensive field-theoretic program took about a decade. Step by step, the Bonn group computed all 2π exchange diagrams including those with virtual Δ-isober excitations and finally, also the relevant diagrams of 3π and 4π exchange. One of the important finding is that, apart from the usual iterative diagrams, the crossed meson exchanges and the diagrams of π and ρ exchange are particularly important for a quantitative description of the NN scattering data and the deuteron properties. The final Bonn model [19] turns out to be highly quantitative nature, in spite of the fact that it employs only about a dozen parameters, such as meson-baryon coupling constants and form factors that have a physical meaning.

There are several reasons for and advantages to a field-theoretic model. First, it determines the off-shell behavior of the interaction in a well-defined way. As dispersion theory deals with reaction amplitudes, which are always on-shell, the off-shell behavior remains undetermined in such an approach and is left to guesswork or arguments of simplicity. Furthermore, the set of diagrams provided by a field-theoretic model forms a sound basis for a consistent generalization to many-body forces, which may be of interest in the nuclear many-body problem. Field-theoretic models also allow for a consistent extension to intermediate energies including meson production.

1.2 The idea of Massive-Particle Exchange:

In the 1930s the best established and most striking feature of the nuclear force was its short-range nature. For that reason, the first theoretical attempts concentrated on deriving a force of finite range from some more fundamental idea. Yukawa achieved this in 1935 by constructing a strict analogy to quantum electrodynamics (QED). His first consideration was carried out in the framework of classical field theory, which we shall now restate.

In QED a field of particles with *zero* mass, the photons, is assumed to fulfill a field equation. In static approximation, the fourth component of this field satisfies the Poisson equation of classical electrodynamics.

$$-\Delta V(\mathbf{r}) = e\delta^{(3)}(\mathbf{r}) \tag{1.2.1}$$

with Δ the Laplace operator. The solution

$$V(r) = \frac{e}{4\pi}\frac{1}{r} \tag{1.2.2}$$

with $r = |\mathbf{r}|$, is the familiar Coulomb potential.

In analogy, in meson theory of field of particles with *nonzero* mass m, the mesons, is assumed, fulfilling a field equation, which is the Klein-Gordon equation (using the units such that $\hbar = c = 1$)

$$(\Box + m^2)\varphi(x) = g\overline{\psi}(x)\psi(x) \tag{1.2.3}$$

In the approximation that the nucleon (the source of the meson field), represented by $\psi(x)$, is infinitely heavy and fixed at the origin, we obtain

$$(-\Delta + m^2)\varphi(\mathbf{r}) = g\delta^{(3)}(\mathbf{r}) \tag{1.2.4}$$

satisfied by the "Yukawa potential"

$$\varphi(r) = \frac{g}{4\pi}\frac{e^{-mr}}{r} \tag{1.2.5}$$

Because of the exponential form, which is a direct consequence of the massive character of the particles, this potential has the desired finite range. For zero mass one recovers the Coulomb potential. This simple consideration, done in 1935, was the birth of particle physics.

Traditionally the range of a particle exchange is estimated from the Compton wavelength equivalent to the particle's mass

$$R = 1/m \tag{1.2.6}$$

In this way, one estimates for the pion (with a mass of 138 MeV) a range of 1.4 fm. This estimate is somewhat small; in fact, the pion just starts to become dominant at that range. That the conventional range estimate is too small is also true for the heavier mesons. It is due to the fact that we are dealing with large coupling constant; the final nuclear potential is a result of strong interferences of large contributions.

1.3 Empirical features of the nuclear force:

We will start to look more closely into meson theory, in qualitative terms, what the meson exchange picture can predict for the NN system. However, first we shall briefly review the empirically known features of the nuclear force. This will later help to better assess the relevance of various meson exchange contributions.

1. **Nuclear forces are of short range (finite range):** That their range is shorter than inter atomic distances we can conclude from the fact that of the molecular level no forces other than electromagnetic ones are needed to explain the known phenomena. However, we can put a much more precise and, in fact, much lower limit on the range by studying closely the saturation properties of nuclei. When going from the A = 4 nucleus, helium, upwards to higher-A nuclei, one realizes that the binding energy per nucleon remains about constant. The density also remains roughly the same, the radius of heavy nuclei being proportional to $A^{1/3}$. If the nuclear force was of long range, like, for example, the coulomb force, the potential energy per particle would increase with A and so would the density. On the other hand, for light nuclei $(A \leq 4)$ the binding energy per nucleon does grow with A. The deuteron is bounded by 2.2 MeV, ^3H by 8.5 MeV. This fact is best analyzed in terms of energy per "bond". Thus, the binding energy per bond is about 2 MeV in the two-nucleon system and 3 Mev for the triton. In ^4He we have ≈ 4.5 MeV per bond (28 MeV total). One can then conclude that, when nucleons are pulled closer to each other by more bonds, also the energy per bond increases (up to saturation). From this Wigner in 1933 conjectured that the nuclear force should be of short range, namely, shorter than the deuteron diameter of about 4 fm and roughly equal to the radius of the alpha particle of about 1.7 fm.

2. **The nuclear force is attractive in its intermediate range:** "Intermediate" is meant here relative to the total range of the nuclear force, which we consider now as being subdivided into short, intermediate and long range. The proof for the attractive character of the nuclear force (at least, in a certain range) is provided by the fact of nuclear binding. The range of this attraction can be obtained more precisely by considering the central density of heavy nuclei as known from electron scattering. This density is about 0.17 fm^{-3} (nuclear matter density), which is equivalent to a cube of length 1.8 fm for each nucleon [8]. Thus the average distance between the centers of two nucleons in the interior of a nucleus is about 1.8 fm, in close agreement with our estimate given above. This average distance should be about the range of the attraction. Further evidence for the

(partially) attractive character of the nuclear force comes from the analysis of NN scattering data. The S-wave phase shifts [8] are positive (corresponding to attraction) for low energies and we note that the average momentum of a nucleon in nuclear matter is equivalent to a laboratory energy of about 50 MeV.

3. **The nuclear force has a repulsive core:** Such an assumption could help to explain the saturation properties of nuclear force and the constant nuclear density. But this aspect is not a compelling proof for repulsive core, as saturation can also be generated in other ways, namely, by "exchange" forces, by Pauli and relativistic effects. In fact, at nuclear matter density the Pauli effect is much more important than the short-range repulsion. However, a precise argument is provided by the behavior of the ${}^1S_0$ and ${}^1D_2$ phase shifts [8] as a function of energy. The latter stays positive (corresponding to attraction) up to about 800 MeV, whereas the ${}^1S_0$ phase shift turns negative (i.e., repulsive) around 250 MeV. Since an S state (orbital angular momentum L = 0, no centrifugal barrier) feels the innermost region of the force, whereas in a D state (L = 2) the nucleons are kept apart by the centrifugal barrier, one may conclude that a repulsion at short range is indicated. The maximum classical orbital angular momentum L_{max} involved in a range R is $L_{max} = Rp$ where the momentum p of a nucleon in the centre of mass frame of the NN system is related to the laboratory energy, E_{lab}, by $E_{lab} = 2p^2/m_N$ with m_N the mass of the nucleon. For E_{lab}=250 MeV, where the ${}^1S_0$ phase shift turns repulsive, we have $p \approx 1.7 fm^{-1}$. With $L_{max} \leq 1$ we obtain $R \leq 0.6 fm$. This should represent a fair estimate of the radius of the repulsive core.

4. **There is a tensor force:** The most striking evidence for this fact is seen in the deuteron: the quadrupole moment, the magnetic moment and the asymptotic D/S state ratio. Further evidence is provided by the nonvanishing mixing parameters, ε_J, as obtained in a phase-shift analysis of NN scattering data [8]. This parameter is proportional to the transition amplitude from a state with

$L = J-1$ to one with $L = J+1$ (with J the total angular momentum). Of all operators, by which the most general non-relativistic potential can be represented, only the tensor operator has non-vanishing matrix elements for this transition.

5. **There is a spin orbit force:** A first indication for this fact was observed in the spectra of nuclei. However, this refers to the effective nuclear interaction in the many-body system, which is not the same as the free NN interaction, though these two forces are related. Clear evidence came from the first reliable phase-shift analysis at high energy [20-22]. The triplet P waves resulting from the analysis can only be explained by assuming a strong spin-orbit force [21-22]. Speaking in terms of observables, a strong spin-orbit force is required to explain the polarization.

1.4 Nuclear matter properties:

By definition, *nuclear matter* refers to an infinite uniform system consisting of an equal number of protons and neutrons interacting through the strong force. The Coulomb interaction is absent and the number of particles, A, approaches infinity. This hypothetical system is supposed to approximate conditions in the interior of a heavy nucleus. We shall assume equal neutron and proton density, that is, we will consider symmetric nuclear matter. This many-body system is characterized by its energy per nucleon as a function of the particle density.

The particle density ρ is constant and the single particle wave functions, or orbitals, are taken to be plane waves. In configuration space the single-particle orbitals, $\phi_\mu(\mathbf{r}_i)$, are given by

$$\phi_\mu(\mathbf{r}_i) = \langle \mathbf{r}_i | \mu \rangle = \frac{\exp i\mathbf{k}_\mu \cdot \mathbf{r}_i}{\Omega^{1/2}} |s_\mu t_\mu\rangle \tag{1.4.1}$$

where s_μ labels the spin state of the nucleon, and t_μ is the isospin label. The nucleons are in the volume Ω, which is used in Eqn. (1.4.1) to normalize the single-particle orbitals. For an infinite system, both A and Ω approach infinity, while the particle density $\rho = A/\Omega$ remains finite.

The ground state of nuclear matter is simply a properly anti-symmetrized product of orbitals with all levels filled, according to the Pauli principle, up to a maximum level specified by k_F, the Fermi momentum. For this state, the total kinetic energy is $\langle T \rangle = \frac{3}{5}\varepsilon_F A$. The Fermi energy and the particle density are respectively given by [3]

$$\varepsilon_F = \left(\hbar^2 / 2m_N\right)k_F^2$$
$$\rho = 2k_F^3 / 3\pi^2 \qquad (1.4.2)$$

The main goal of nuclear matter calculations is to determine the saturation curve, i.e. the binding energy per nucleon as a function of density. The equilibrium binding energy and density are determined by finding a minimum in the saturation curve. The basic saturation condition placed on a potential by nuclear matter is that the correct binding energy and density be obtained.

Empirical information of the minimum of that curve, the saturation point, is deducted by extrapolation from the properties of finite nuclei. Based on the liquid drop model for the nucleus, the semi-empirical Bethe-Weizacker mass formula provides a value for the energy via its volume term. A collection of contemporary mass formulas by many different authors can be found in the *Atomic Data and Nuclear Data Tables* [23]. From the charge distribution of heavy nuclei as determined in electron scattering, the saturation density can be deduced by taking into account corrections due to the Coulomb repulsion and the surface tension. Alternatively, both the saturation energy and density can be deduced from Hartree-Fock or Thomas-Fermi calculations [24-28] with phenomenological effective forces fitted to the ground-state properties of closed-shell nuclei. Thus, nuclear matter is determined to saturate at a density

$$\rho_0 = 0.17 \pm 0.02\, fm^{-3} \qquad (1.4.3)$$

and binding energy per nucleon

$$\varepsilon / A = -16 \pm 1 \text{ MeV} \qquad (1.4.4)$$

Other parameters related to the particle density are the inter-particle spacing r and the Fermi momentum k_F which are defined by

$$4\pi r^3/3 = 1/\rho \tag{1.4.5}$$

and

$$k_F = \left[3\pi^2 \rho(r)/2\right]^{1/3} \tag{1.4.6}$$

At the saturation point the equilibrium values for these quantities corresponding to the above given ρ_0 are

$$r_0 = 1.3 \pm 0.04 fm \tag{1 4.7}$$

$$k_F = 1.35 \pm 0.05 fm^{-1} \qquad \text{at } \rho = \rho_0 \tag{1.4.8}$$

Also of interest is the incompressibility or compression modulus of saturated nuclear matter

$$K = k_F^2 \frac{\partial^2[\varepsilon/A(k_F)]}{\partial k_F^2} \tag{1.4.9}$$

evaluated at k_F given in Eqn. (1.4.8) From empirical information deduced from the systematic vibrations in nuclei [8], one obtains for the saturation point.

$$K = 210 \pm 30 \text{ MeV} \tag{1.4.10}$$

In many-body calculations using density-dependent phenomenological forces fit to the groundstate properties of closed-shell nuclei, values for the compressions modulus are obtained which agree with Eqn. (1.4.10).

Chapter-2

Boson fields and One-boson exchange potentials

In this chapter, we first consider the meson-exchange contribution in the framework of perturbation theory and describe the Feynman rules for calculating the scattering amplitude for free nucleus-nucleus interaction. Then we discuss some simple relevant boson fields and their couplings in one-boson-exchange contribution, in section two. Finally, in section three, we use the standard interaction Lagrangian for each field and with the help of Feynman rules we construct the one-boson-exchange potentials of the Bonn type and discuss their role in NN interaction.

2.1 Perturbation theory and Feynman rules

The first meson-theoretic consideration was done in the framework of classical field theory. For more advanced considerations, quantized field theory should be applied. This field theory was developed first for QED. The interactions involved are treated perturbatively and are most conveniently represented in terms of Feynman diagrams. Originally, meson theory was believed to represent the theory of strong interaction in analogy to QED. Nowadays, with QCD being the theory for strong interactions, meson theory is viewed as an effective description, which may represent the appropriate approximation to the full and fundamental theory in the low-energy regime. It is customary to consider meson-baryon reactions in terms of perturbation theory and consequently, to consider the various possible contributions in the graphical language of Feynman diagrams. Contributions of increasing order, which may finally become divergent, are of shorter and shorter range. For the long and intermediate range, there is only a finite number of perturbative contributions. Thus for these ranges one may have confidence in the predictions generated by perturbation theory. At the very short-range part of the force, due to the quark-structure of hadrons, the meson-exchange picture cannot be taken seriously. For that reason, in most meson theories, one allows for a partly phenomenological treatment of the short distances by the introduction of vertex form factors, which in a certain sense, takes the extended structure of hadrons effectively into account. Fortunately, since the nuclear force is repulsive at short internucleonic distances, the phenomenology of the very short range is "masked" behind a repulsive wall. Thus, one expects that, at least for energies typical for nuclear physics, the uncertain part of the nuclear force at very short distances and the special way, in which it may be treated in a particular model, is insignificant.

For the above reasons, we follow here the conventional treatment and consider meson-exchange in the framework of perturbation theory; that is, more practically speaking, we will be dealing with Feynman diagrams.

In a scattering theory the problem is to find the amplitude, which contains all the dynamical information. Evaluating the relevant Feynman diagrams and using the Feynman rules appropriate to the interaction in question can solve this problem. The rules are summarized as follows [29].

1. **Notation:** Label the incoming and outgoing four-momenta $q_1, q_2, \ldots\ldots\ldots\ldots\ q_n$ and the corresponding spins $s_1, s_2, \ldots\ldots\ldots\ldots s_n$, label the internal four-momenta $k_1, k_2, \ldots\ldots\ldots k_n$. Assign arrows to the lines as follows: the arrows on external lines indicate whether it is incoming or outgoing; arrows on internal lines are assigned so that the "direction of the flow" through the diagram is preserved (i.e. every vertex must have one arrow entering and one arrow leaving). Put an arrow on each line. to keep track of the positive direction (arbitrarily assigned, for the internal lines).

2. **External lines:** External lines contribute factors as follows:

   Spin 0 : Nothing

   Spin 1/2 : Incoming particle: u

   Outgoing particle: $\bar{u}$

   Incoming antiparticle: $\bar{v}$

   Outgoing antiparticle: v

   Spin 1 : Incoming: ε^{μ}

   Outgoing: ε^{μ^*}

3. **Propagators:** Each internal line contributes a factor as follows:

Spin 0 : $\dfrac{i}{k^2 - m_\alpha^2}$

Spin $\dfrac{1}{2}$: $\dfrac{i(k + m_\alpha)}{k^2 - m_\alpha^2}$

Spin 1 : Massless: $\dfrac{-ig_{\mu\nu}}{k^2}$

Massive: $\dfrac{-i\left(g_{\mu\nu} - k_\mu k_\nu / m_\alpha^2\right)}{k^2 - m_\alpha^2}$

where $g_{\mu\nu}$ is the metric tensor with $g_{00} = +1$, $g_{kk} = -1$ and $g_{\mu\neq\nu} = 0$.

4. **Vertex Factors:** Each vertex contributes a factor $g_i\Gamma_i$ where g is called the coupling constant which is dimensionless. Furthermore, there is a factor of i in each vertex.

5. **Conservation of energy and momentum:** For each vertex, write a delta function of the form $(2\pi)^4\delta^4(q_1 + q_2 + q_3)$ where q's are the three four-momenta coming into the vertex (if an arrow leads outward, then q is minus the four-momentum of that line). This factor enforces conservation of energy and momentum at each vertex.

6. **Integration over internal momenta:** For each internal line, write down a factor $\dfrac{1}{(2\pi)^4}d^4k_j$ and integrate over all internal momenta.

7. **Cancel the delta function:** The result will include a delta function $(2\pi)^4\delta^4(q_i + q_2 + \dots\dots\dots\dots + q_n)$ enforcing overall conservation of energy and momentum. Cancel this factor, and what remains is $-i\mathcal{M}$ where $\mathcal{M}$ is the scattering amplitude.

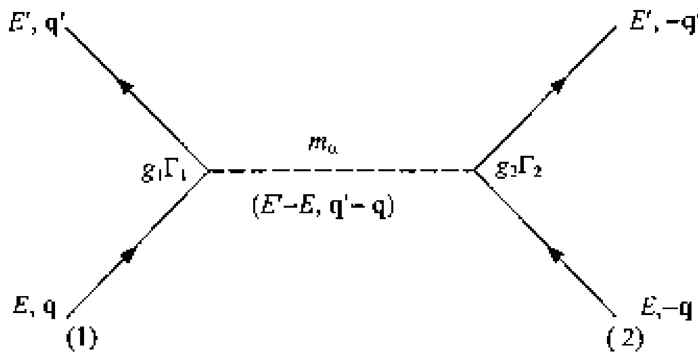

Fig.2.1: Feynman diagram for the one-boson-exchange contribution to NN scattering considered in the c.m. frame. Full lines denote nucleons, the dashed line a boson with mass m_α. The underlying time axis is vertical, pointing upwards into the future.

The lowest-order contribution to the NN scattering is the one-boson-exchange contribution. The respective Feynman diagram is depicted in Fig.2.1. Since we are working in the center of mass (c.m.) system of the two interacting nucleons, the momenta of the two incoming particles are $\mathbf{q}$ and $-\mathbf{q}$ and those for the outgoing particles are $\mathbf{q}'$ and $-\mathbf{q}'$. The process takes place "on the energy shell' i.e. energy is conserved; consequently the energy of the nucleons before, E, and after E', the scattering process must be same so that $E' = E$.

According to the "Feynman rules" the depiction in Fig 2.1 corresponds to the scattering amplitude in analytic form:

$$\frac{g_1\bar{u}_1(\mathbf{q}')\Gamma_1 u_1(\mathbf{q})P_\alpha g_2\bar{u}_2(-\mathbf{q}')\Gamma_2 u_2(-\mathbf{q})}{(q'-q)^2 - m_\alpha^2} \tag{2.1.1}$$

where the left half of the numerator represents the left part of the diagram and the right half for the right part of the diagram. u_i and $\bar{u}_i\left(\equiv u_i^\dagger\gamma^0\right)$ are Dirac spinors and their adjoints representing incoming and outgoing nucleons, respectively, with $i = 1$ and 2. The meson propagator represented by the dashed line in the figure is

$$\frac{P_\alpha}{(q'-q)^2 - m_\alpha^2} \tag{2.1.2}$$

where $(q'-q)^2 = (E'-E)^2 - (\mathbf{q}'-\mathbf{q})^2 = -(\mathbf{q}'-\mathbf{q})^2$, is the square of the four-momentum transferred by the meson. Thus we have for the propagator

$$\frac{P_\alpha}{-(\mathbf{q}'-\mathbf{q})^2 - m_\alpha^2} \tag{2.1.3}$$

For scalar and pseudoscalar exchanges $P_\alpha = i \equiv \sqrt{-1}$. For vector boson exchange, however, it is:

$$P_\alpha = -i\left(g_{\mu\nu} - \frac{k_\mu k_\nu}{m_\alpha^2}\right) \tag{2.1.4}$$

Since the vector bosons couple to a conserved nucleon current the second term will become zero in the actual calculations. Thus we can use for vector-boson exchange:

$$P_\alpha = -ig_{\mu\nu} \tag{2.1.5}$$

The last pieces $g_i\Gamma_i$ are the "vertices" representing meson-nucleon interactions and are obtained from the interaction Lagrangians. In fact, logically we should have begun with the interaction Lagrangians, as they are the starting point for the development of the field theoretic perturbation theory, the lowest order result of which (for NN and excluding renormalization) is our Feynman diagram Fig. 2.1. In any case, the respective interaction Lagrangians for Fig.2.1 are

$$\mathcal{L}_i = g_i \overline{\psi}\,\Gamma_i \psi\, \varphi^{(\alpha)}; \qquad i = 1, 2 \tag{2.1.6}$$

Where $(\overline{\psi})\psi$ is the (adjoint) nucleon Dirac field and $\varphi^{(\alpha)}$ the meson field operator. Comparison of Eqn.(2 1.6) with Eqn.(2.1.1) shows in an obvious way, how to obtain the vertex from a Lagrangian in a simple case. We note that the vertex is i times the interaction Lagrangian stripped off the fields and that i times the amplitude in Eqn. (2.1.1) defines the potential V_α .

2.2 Various Boson fields and their couplings:

In this section we go systematically through some of the simplest boson fields and their couplings. In each case we consider the one-boson-exchange diagram and derive from it explicitly what it predicts for the NN interaction. For the NN interaction at low energy there are essentially only four boson fields that are of relevance:

1) The pseudoscalar (ps) field
2) The pseudovector (pv) field
3) The scalar (s) field
4) The vector (v) field.

Guided by symmetry principles, simplicity and physical interaction, the most commonly used interaction Lagrangians that couple these fields to the nucleon are [8]

$$\mathcal{L}_{ps} = -g_{ps}\overline{\psi}\, i\gamma^5 \psi\, \varphi^{(ps)} \tag{2.2.1}$$

$$\mathcal{L}_{pv} = -\frac{f_{ps}}{m_{ps}}\overline{\psi}\,\gamma^5\gamma^\mu\psi\,\partial_\mu\varphi^{(ps)} \tag{2.2.2}$$

$$\mathcal{L}_s = g_s\overline{\psi}\psi\,\varphi^{(s)} \tag{2.2.3}$$

$$\mathcal{L}_v = -g_v\overline{\psi}\gamma^\mu\psi\,\varphi_\mu^{(v)} - \frac{f_v}{4m_N}\overline{\psi}\sigma^{\mu\nu}\psi\left(\partial_\mu\varphi_\nu^{(v)} - \partial_\nu\varphi_\mu^{(v)}\right) \tag{2.2.4}$$

where ψ denotes the nucleon Dirac spinor field, while $\varphi^{(ps)}$, $\varphi^{(s)}$ and $\varphi^{(v)}$ are the pseudoscalar, scalar and vector boson fields respectively; m_N is the nucleon mass. In Eqn. (2.2.4) the first term on the right-hand side is called the vector (v) and the second term the tensor (t) coupling. Also

$$\gamma^0 = \begin{pmatrix} 1 & 0 \\ 0 & -1 \end{pmatrix},\ \gamma^k = \begin{pmatrix} 0 & \sigma^k \\ -\sigma^k & 0 \end{pmatrix},\ \gamma_5 = \gamma^5 = i\gamma^0\gamma^1\gamma^2\gamma^3 = \begin{pmatrix} 0 & 1 \\ 1 & 0 \end{pmatrix} \text{ and } \sigma^{\mu\nu} = \frac{i}{2}\left[\gamma^\mu, \gamma^\nu\right]$$

where σ^k are the usual Pauli spin matrices. The Greek indices extend from 0 to 3 and the Latin indices from 1 to 3.

For ps field there is the so-called pseudovector (pv) or gradient coupling, Eqn. (2.2.2), to the nucleon, which is an effective coupling by chiral symmetry [30, 31]. The ps and pv coupling are equivalent for on-mass-shell nucleons if the coupling constants are related by $f_{ps} = (m_{ps}/2m_N)g_{ps}$. However, the off-shell predictions are rather different. The Lagrangians mentioned lead to the following (off-shell) OBE amplitudes:

$$\left\langle \mathbf{q}'\lambda_1'\lambda_2' \middle| V_{ps}^{OBE} \middle| \mathbf{q}\lambda_1\lambda_2 \right\rangle = -g_{ps}^2 \bar{u}(\mathbf{q}',\lambda_1') i\gamma^5 u(\mathbf{q},\lambda_1) \bar{u}(-\mathbf{q}',\lambda_2') i\gamma^5 u(-\mathbf{q},\lambda_2) \left[(\mathbf{q}'-\mathbf{q})^2 + m_{ps}^2\right]^{-1} \tag{2.2.5}$$

$$\left\langle \mathbf{q}'\lambda_1'\lambda_2' \middle| V_{pv}^{OBE} \middle| \mathbf{q}\lambda_1\lambda_2 \right\rangle = \frac{f_{ps}^2}{m_{ps}^2} \bar{u}(\mathbf{q}',\lambda_1') \gamma^5 \gamma^\mu i(q'-q)_\mu u(\mathbf{q},\lambda_1)$$

$$\times \bar{u}(-\mathbf{q}',\lambda_2') \gamma^5 \gamma^\mu i(q'-q)_\mu u(-\mathbf{q},\lambda_2) \left[(\mathbf{q}'-\mathbf{q})^2 + m_{ps}^2\right]^{-1} \tag{2.2.6}$$

$$\left\langle \mathbf{q}'\lambda_1'\lambda_2' \middle| V_s^{OBE} \middle| \mathbf{q}\lambda_1\lambda_2 \right\rangle = -g_s^2 \bar{u}(\mathbf{q}',\lambda_1') u(\mathbf{q},\lambda_1) \bar{u}(-\mathbf{q}',\lambda_2') u(-\mathbf{q},\lambda_2) \left[(\mathbf{q}'-\mathbf{q})^2 + m_s^2\right]^{-1} \tag{2.2.7}$$

$$\left\langle \mathbf{q}'\lambda_1'\lambda_2' \middle| V_v^{OBE} \middle| \mathbf{q}\lambda_1\lambda_2 \right\rangle = \left\{ g_v \bar{u}(\mathbf{q}',\lambda_1') \gamma_\mu u(\mathbf{q},\lambda_1) + \frac{f_v}{2m_N} \bar{u}(\mathbf{q}',\lambda_1') \sigma_{\mu\nu} i(q'-q)^\nu u(\mathbf{q},\lambda_1) \right\}$$

$$\times \left\{ g_v \bar{u}(-\mathbf{q}',\lambda_2') \gamma^\mu u(-\mathbf{q},\lambda_2) - \frac{f_v}{2m_N} \bar{u}(-\mathbf{q}',\lambda_2') \sigma^{\mu\nu} i(q'-q)_\nu u(-\mathbf{q},\lambda_2) \right\}$$

$$\times \left[(\mathbf{q}'-\mathbf{q})^2 + m_v^2\right]^{-1} \tag{2.2.8}$$

where $\lambda_i(\lambda_i')$ denotes the helicity of an incoming (outgoing) nucleon, which is defined as the eigenvalue of the operator $\mathbf{s}\cdot\hat{\mathbf{q}}$ with $\mathbf{s}$ the spin operator and $\hat{\mathbf{q}} = \mathbf{q}/|\mathbf{q}|$ the unit momentum operator of the respective nucleon; $E = \left(m_N + \mathbf{q}^2\right)^{1/2}$ and $E' = \left(m_N + \mathbf{q}'^2\right)^{1/2}$. The Thompson choice for the four-momentum transfer i. e. $(q'-q) = (0, \mathbf{q}'-\mathbf{q})$ is made. It is now in principle a straightforward (but quite lengthy) task to evaluate the one-boson-exchange contributions, Eqn. (2.1.1), corresponding to the interaction Lagrangians given above, which is done in the next section. This will reveal what each field and coupling predicts for the nuclear force.

2.3 One-Boson exchange potentials and their contribution in NN interaction:

The one-boson exchange potential (OBEP) is defined as a sum of one-particle exchange amplitudes of certain bosons with given mass and coupling. In the OBE Bonn model six non-strange bosons with mass below 1 GeV are used; they are π and η pseudoscalar, σ and δ scalar and ρ and ω vector mesons. Thus

$$V_{OBEP} = \sum_{\alpha=\pi,\eta,\rho,\varpi,\delta,\sigma} V_{\alpha}^{OBE} \qquad (2.3.1)$$

The contributions from the isovector bosons, π, δ and ρ are to be multiplied by a factor of $\tau_1 \cdot \tau_2$. For isospin -1, the mesons $\varphi^{(\alpha)}$ is to be replaced by $\tau \cdot \varphi^{(\alpha)}$, with τ^k (k = 1,2,3) the usual Pauli matrices.

Now we evaluate the OBE contributions, Eqn. (2.1.1), corresponding to the interaction Lagrangians given above with ψ the nucleon and $\varphi^{(\alpha)}$ the meson fields. Strictly speaking, we give here the potential that is defined as i times the Feynman amplitude. Furthermore, there is a factor of 'i' in each vertex and meson propagator; as $i^4 = 1$, we can ignore these four factors of 'i'.

The pseudoscalar (ps) field:

Pseudoscalar means the field, $\varphi^{(ps)}$, switches sign in the case of either space or a time reflection. Particles with negative intrinsic parity, e.g. the π and η , have this property To "counterbalance" this we have to find an expression $\bar{\psi}\Gamma\psi$, which has the same property as $\varphi^{(ps)}$, to obtain a scalar for the whole expression for the interaction Lagrangian. The simplest case with this property is $\bar{\psi}\gamma^5\psi$. Thus

$$\mathcal{L}_{ps} = -g_{ps}\bar{\psi}\, i\gamma^5\psi\, \varphi^{(ps)}. \qquad (2.3.2)$$

(The i is needed for the hermiticity, as γ^0 and γ^5 anti-commute). The one-boson-exchange (OBE) contribution V_{ps}^{OBE}, for this interaction is according to Feynman rules, Fig 2.1 and Eqn. (2.1.1):

$$\frac{g_{ps}^2\bar{u}_1(\mathbf{q}')i\gamma^5 u_1(\mathbf{q})\bar{u}_2(-\mathbf{q}')i\gamma^5\bar{u}_2(-\mathbf{q})}{-(\mathbf{q}'-\mathbf{q})^2-m_{ps}^2} \tag{2.3.3}$$

where the incoming nucleons are represented by the Dirac spinors u_1 and u_2 given by

$$u_1(\mathbf{q})=\sqrt{\frac{E+m_N}{2E}}\begin{pmatrix}1\\ \frac{\sigma_1.\mathbf{q}}{E+m_N}\end{pmatrix} \text{ and } u_2(-\mathbf{q})=\sqrt{\frac{E+m_N}{2E}}\begin{pmatrix}1\\ \frac{\sigma_2.\mathbf{q}}{E+m_N}\end{pmatrix} \tag{2.3.4}$$

Here and in the following we suppress spin-indices and spin·functions. The outgoing nucleons are represented by the adjoint Dirac spinors $\bar{u}_1$ and $\bar{u}_2$; the normalization of the Dirac spinor being $u_i^\dagger(\mathbf{q})u_i(\mathbf{q})=1$. So

$$\bar{u}_1(\mathbf{q})=u_1^\dagger(\mathbf{q})\gamma^0=\left(\frac{E+m_N}{2E}\right)^{\frac{1}{2}}\begin{pmatrix}1 & \frac{-\sigma_1.\mathbf{q}}{E+m_N}\end{pmatrix}$$

Now the left half of the numerator is

$$\bar{u}_1(\mathbf{q}')i\gamma^5 u_1(\mathbf{q})=i\sqrt{\frac{(E+m_N)(E'+m_N)}{4EE'}}\begin{pmatrix}\frac{\sigma_1\cdot\mathbf{q}}{E+m_N} & \frac{-\sigma_1.\mathbf{q}'}{E'+m_N}\end{pmatrix}$$

"On the shell" model, we use $E=E'$. So we obtain

$$\bar{u}_1(\mathbf{q}')i\gamma^5 u_1(\mathbf{q})=\frac{i}{2E}\sigma_1.(\mathbf{q}-\mathbf{q}') \tag{2.3.5}$$

Similarly, for the right half of the numerator

$$\bar{u}_2(-\mathbf{q}')i\gamma^5 u_2(-\mathbf{q})=\frac{i}{2E}\sigma_2.(\mathbf{q}'-\mathbf{q}) \qquad \text{(for the "on-shell")}$$

Putting everything together, we obtain for the whole diagram the following "momentum space potential":

$$V_{ps}(\mathbf{q}',\mathbf{q})=\frac{g_{ps}^2}{-(\mathbf{q}'-\mathbf{q})^2-m_{ps}^2}\frac{i}{2E}\sigma_1(\mathbf{q}-\mathbf{q}')\frac{i}{2E}\sigma_2.(\mathbf{q}'-\mathbf{q}), \qquad \text{giving}$$

$$V_{ps}(\mathbf{k})=-\frac{g_{ps}^2}{4m_N^2}\frac{(\sigma_1\cdot\mathbf{k})(\sigma_2\cdot\mathbf{k})}{\mathbf{k}^2+m_{ps}^2} \tag{2.3.6}$$

where the momentum transfer $\mathbf{q}'-\mathbf{q}=\mathbf{k}$ has been used and the approximation $E\approx m_N$ is assumed. We may rewrite the above expression as

$$V_{ps}(\mathbf{k})=-\frac{1}{12m_N^2}\frac{g_{ps}^2}{\mathbf{k}^2+m_{ps}^2}\mathbf{k}^2\left[\sigma_1\cdot\sigma_2+\mathbf{S}_{12}(\mathbf{k})\right] \tag{2.3.7}$$

where $S_{12}(\mathbf{k}) = 3(\sigma_1 \cdot \mathbf{k})(\sigma_2 \cdot \mathbf{k}) - \sigma_1 . \sigma_2$ has been used. The above expression shows that it becomes obvious that we have created a spin-spin and a tensor force.

The best known pseudoscalar field is the pion. There exist three charge states of the pion: +, –, neutral or with other words, its isospin is one; it is an isovector particle. In such a case the Lagrangian in Eqn. (2.2.1) is slightly extended:

$$\mathcal{L}_{ps} = -g_{ps}\overline{\psi} i\gamma^5 \boldsymbol{\tau}\psi \cdot \boldsymbol{\varphi}^{(ps)} \tag{2.3.8}$$

where the three components of $\boldsymbol{\varphi}^{(ps)}$ are operators in isospin space, as there are now three charged states. $\boldsymbol{\tau}$ is the usual isospin operator for isospin $1/2$ particles, here the nucleons. $\boldsymbol{\tau}\cdot\boldsymbol{\varphi}^{(ps)}$ is an invariant in isospin space. By that, the charge-independence of the interaction is guaranteed. As a consequence, for isovector particle exchange, the Feynman diagram Eqn. (2.2.5) and the potential derived in Eqn.(2.3.6) obtain a factor $\boldsymbol{\tau}_1.\boldsymbol{\tau}_2$

$$V_{ps}(\mathbf{k}) = -\frac{g_{ps}^2}{4m_N^2}\frac{(\sigma_1 \cdot \mathbf{k})(\sigma_2 \cdot \mathbf{k})}{\mathbf{k}^2 + m_{ps}^2}\ \boldsymbol{\tau}_1.\boldsymbol{\tau}_2 \tag{2.3.9}$$

In summary, we started with a boson field for which we assumed that it was pseudoscalar (equivalent to a particle with negative intrinsic parity which is observed in nature e.g. for π, η). Consequently, we had to use the γ^5-coupling (as the simplest possibility to comply with certain indispensable symmetries). A small calculation then leads directly to a tensor force. In this way it is easily understood that, starting from first principles, the pion creates a tensor force.

We also note that the γ^5-coupling projects small components of the Dirac spinors onto large components, Eqn. (2.3.5). Therefore, it is, in its analytical structure, a "weak" coupling. The reason, why the pion, nevertheless, is non-negligible, is the small mass of the pion, which strengthens the potential (note that the meson mass squared appears in the denominator of the Feynman diagram, Eqn. (2.1.1)). In fact, the simple rule of thumb, to roughly compare the strength of two OBE contributions of the same kind, is to consider:

$$\frac{g_\alpha^2}{m_\alpha^2}$$

From this argument it is now obvious that a heavy *ps*-particle leads to very small contributions. Examples are the $\eta\,(m_\eta = 549\,\mathrm{MeV})$ and the $\eta'\,(m_{\eta'} = 958\ \mathrm{MeV})$.

We mentioned before that for a certain field, in general, several (in principle infinitely many) couplings are possible. So, for a *ps*-field a derivative coupling is also commonly considered, the pseudovector (*pv*) coupling:

$$\mathcal{L}_{pv} = -\frac{f_{ps}}{m_{ps}} \bar{\psi}\gamma^5\gamma^\mu\psi\,\partial_\mu\varphi^{(ps)} \tag{2.3.10}$$

The resulting left vertex is

$$\Gamma_{pv} = \frac{f_{ps}}{m_{ps}} i\gamma^5\gamma^\mu (q'-q)_\mu \tag{2.3.11}$$

($i\partial_\mu$ is the momentum operator; $(q'-q)_\mu$ the four-momentum of the exchanged meson.) Application in the Feynman diagram, Eqn.(2.1.1), leads, in the numerator, to expressions like $\gamma^\mu q_\mu u_1(\mathbf{q})$ and $\bar{u}_1(\mathbf{q}')\gamma^\mu \mathbf{q}'_\mu$. The Dirac equation allows us to write

$$\gamma^\mu q_\mu u_1(\mathbf{q}) = m_N u_1(\mathbf{q}) \tag{2.3.12}$$

$$\bar{u}_1(\mathbf{q}')\gamma^\mu q'_\mu = m_N \bar{u}_1(\mathbf{q}') \tag{2.3.13}$$

With these replacements the upper left part of the Feynman diagram becomes

$$\frac{f_{ps}}{m_{ps}} i\bar{u}_1(\mathbf{q}')\gamma^5\gamma^\mu (q'-q)_\mu u_1(\mathbf{q})$$

$$= i\frac{f_{ps}}{m_{ps}}\left[\bar{u}_1(\mathbf{q}')\gamma^5\gamma^\mu q'_\mu u_1(\mathbf{q}) - \bar{u}_1(\mathbf{q}')\gamma^5\gamma^\mu q_\mu u_1(\mathbf{q})\right]$$

$$= i\frac{f_{ps}}{m_{ps}}\left[-\bar{u}_1(\mathbf{q}')\gamma^\mu\gamma^5 q'_\mu u_1(\mathbf{q}) - \bar{u}_1(\mathbf{q}')\gamma^5\gamma^\mu q_\mu u_1(\mathbf{q})\right]$$

[since γ^5 and γ^μ anticommute]

$$= -i\frac{f_{ps}}{m_{ps}}\left[m_N\bar{u}_1(\mathbf{q}')\gamma^5 u_1(\mathbf{q}) + m_N\bar{u}_1(\mathbf{q}')\gamma^5 u_1(\mathbf{q})\right] \quad \text{(using Dirac equation)}$$

$$= -f_{ps}\frac{2m_N}{m_{ps}}\bar{u}_1(\mathbf{q}')i\gamma^5 u_1(\mathbf{q}) \tag{2.3.14}$$

When compared to Eqn. (2.3.3) it turns out that this is exactly the same result as for *ps* coupling, provided we relate the coupling constants as

$$g_{ps} = f_{ps}\frac{2m_N}{m_{ps}} \tag{2.3.15}$$

In this consideration, the nucleons are on their mass shell. In such a case the Dirac equations, Eqn. (2.3.12) and Eqn. (2.3.13), apply, and we see that, then, the *ps* and *pv* couplings are equivalent. For off-shell this is not in general true.

As *ps* and *pv* couplings are equivalent on-shell, we can derive our non-relativistic form of OBE contribution V_{pv}^{OBE} also by starting from the *pv* coupling Eqn. (2.3.10) and proceed as follows; let us consider only the important part of the vertex Eqn. (2.3.11):

$$\Gamma_{pv} = \gamma^5\gamma^\mu k_\mu \quad = \gamma^5\gamma^0 k_0 + \gamma^5\gamma^i k_i$$
$$= \begin{pmatrix} \sigma\cdot\mathbf{k} & 0 \\ 0 & -\sigma\cdot\mathbf{k} \end{pmatrix} \tag{2.3.16}$$

where $\quad k = q' - q\,,\quad k_0 = E' - E = 0$

Some simple rules of non-relativistic reduction are

$$i\partial_\mu = i\frac{\partial}{\partial x^\mu} \to \pm\mathbf{k}\,,\quad \gamma^5\gamma^\mu \to -\sigma\,,\quad \sigma^{\mu\nu} \to \sigma\times \tag{2.3.17}$$

and replacing Dirac spinors by Pauli spinors. Non-relativistic approximation also means assuming $|\mathbf{q}|,|\mathbf{q}'| \leq m_N$ and therefore neglecting the small components in the Dirac spinor;

$$u_1(\mathbf{q}) \approx \begin{pmatrix} 1 \\ 0 \end{pmatrix}; \qquad \bar{u}_1(\mathbf{q}') \approx (1 \quad 0) \tag{2.3.18}$$

Sandwiching the vertex Eqn. (2.3.16) with these Pauli spinors and recollecting the constant factors yields:

$$\bar{u}_1(\mathbf{q}')\Gamma_{pv}u(\mathbf{q}) \approx -i\frac{f_{ps}}{m_{ps}}(\sigma\cdot\mathbf{k}) \tag{2.3.19}$$

Repeating the same consideration for the right vertex (the momentum carries an opposite sign on the right) we get

$$i\frac{f_{ps}}{m_{ps}}(\sigma\cdot\mathbf{k})$$

which leads to the momentum space OBE contribution V_{pv}^{OBE} as

$$-\frac{f_{ps}^2}{m_{ps}^2}\frac{(\sigma_1\cdot\mathbf{k})(\sigma_2\cdot\mathbf{k})}{\mathbf{k}^2 + m_{ps}^2}$$

using Eqn. (2.3.15), we get

$$-\frac{g_{ps}^2}{4m_N^2}\frac{(\sigma_1\cdot\mathbf{k})(\sigma_2\cdot\mathbf{k})}{\mathbf{k}^2+m_{ps}^2} \tag{2.3.20}$$

which is same as Eqn. (2.3.6). In this way the non-relativistic character of the derivation is more obvious.

The scalar(s) field:

This field has the simplest interaction Lagrangian for meson nucleon coupling:

$$\mathcal{L}_s = g_s\overline{\psi}\psi\varphi_s$$

The one-scalar-boson exchange contribution is :

$$g_s^2\frac{\overline{u}_1(\mathbf{q}')u_1(\mathbf{q})\overline{u}_2(-\mathbf{q}')u_2(-\mathbf{q})}{-(\mathbf{q}'-\mathbf{q})^2-m_s^2} \tag{2..3.21}$$

The left half of the numerator:

$$\overline{u}_1(\mathbf{q}')u_1(\mathbf{q}) = \sqrt{\frac{(E'+m_N)(E+m_N)}{4EE'}}\left(1-\frac{(\sigma_1.\mathbf{q}')(\sigma_1.\mathbf{q})}{(E'+m_N)(E+m_N)}\right) \tag{2.3.22}$$

Now we use the vector identity $(\sigma\cdot\mathbf{a})(\sigma\cdot\mathbf{b}) = \mathbf{a}\cdot\mathbf{b}+i\sigma.(\mathbf{a}\times\mathbf{b})$ for the term $(\sigma_1\ \mathbf{q}')(\sigma_1.\mathbf{q})$;

$$(\sigma_1\cdot\mathbf{q}')(\sigma_1.\mathbf{q}) = (\mathbf{q}'\cdot\mathbf{q})+i\sigma_1\cdot(\mathbf{q}'\times\mathbf{q}) = \mathbf{p}^2-(1/4)\mathbf{k}^2+i\sigma_1\cdot(\mathbf{q}'\times\mathbf{q}) \tag{2.3.23}$$

where the momentum variable $\mathbf{p}=\frac{1}{2}(\mathbf{q}'+\mathbf{q})$ and the momentum transfer $\mathbf{k}=\mathbf{q}'-\mathbf{q}$ have been used.

Again, since $\mathbf{k}\times\mathbf{p} = (\mathbf{q}'-\mathbf{q})\times\frac{1}{2}(\mathbf{q}'+\mathbf{q}) = \mathbf{q}'\times\mathbf{q}$, we obtain

$$\overline{u}_1(\mathbf{q}')u_1(\mathbf{q}) = \sqrt{\frac{(E'+m_N)(E+m_N)}{4EE'}}\left\{1-\frac{\mathbf{p}^2-(1/4)\mathbf{k}^2+i\sigma_1.(\mathbf{k}\times\mathbf{p})}{(E'+m_N)(E+m_N)}\right\}$$

$$=\left\{1-\frac{\mathbf{p}^2-(1/4)\mathbf{k}^2+i\sigma_1.(\mathbf{k}\times\mathbf{p})}{4m_N^2}\right\} \quad (\text{assuming } E'\approx E\approx m_N) \tag{2.3.24}$$

Similarly for the right half of the numerator we get

$$\overline{u}_1(-\mathbf{q}')u_1(-\mathbf{q}) = \left\{1-\frac{\mathbf{p}^2-(1/4)\mathbf{k}^2+i\sigma_2.(\mathbf{k}\times\mathbf{p})}{4m_N^2}\right\} \tag{2.3.25}$$

Now the final result for the whole diagram, we obtain the following momentum space potential,

$$V_s(\mathbf{k}\cdot\mathbf{P}) = \frac{-g_s^2}{\mathbf{k}^2+m_s^2}\left[1-\frac{\mathbf{p}^2}{2m_N^2}+\frac{\mathbf{k}^2}{8m_N^2}-\frac{i}{2m_N^2}\frac{1}{2}(\sigma_1+\sigma_2)(\mathbf{k}\times\mathbf{p})\right]$$

$$=\frac{-g_s^2}{\mathbf{k}^2+m_s^2}\left[1-\frac{\mathbf{p}^2}{2m_N^2}+\frac{\mathbf{k}^2}{8m_N^2}-\frac{i}{2m_N^2}\mathbf{S}\cdot(\mathbf{k}\times\mathbf{p})\right];\ \text{where } \mathbf{S}=\frac{1}{2}(\sigma_1+\sigma_2) \qquad (2.3.26)$$

The first term on the right hand side is a strong attractive central force, the last term a spin-orbit force. So the scalar meson-exchange causes a strong attractive central force and a spin-orbit force. From the explicit derivation we realize that the strong central force is due to the fact that the scalar coupling projects large components of the Dirac spinors on large components. The negative over-all sign is a consequence of having a second order in the coupling constant. The spin-orbit force can be traced back to the small components of the Dirac spinors. Therefore, it is a genuine relativistic effect.

The vector (v) field:

A vector boson has spin one, like a photon, and is represented by a four-vector field. To form a Lorentz scalar one can couple it to another four vector, in analogy to the coupling of a photon to an electron:

$$L_v = -g_v\overline{\psi}\gamma^\mu\psi\varphi_\mu^v + \frac{if_v}{2m_N}\overline{\psi}\sigma^{\mu\nu}\psi\,\partial_\mu\varphi_\nu^{(v)} \qquad (2.3.27)$$

The evaluation of one-vector-boson exchange contribution is:

$$\left(-g_v\overline{u}_1(\mathbf{q}')\gamma^\mu u_1(\mathbf{q})+i\frac{f_v}{2m_N}\overline{u}_1(\mathbf{q}')\sigma^{\mu\nu}(\mathbf{q}'-\mathbf{q})_\mu u_1(\mathbf{q})\right)$$

$$\times\frac{(-g_{\mu\nu})}{-(\mathbf{q}'-\mathbf{q})^2-m_v^2}\quad\left(-g_v\overline{u}_2(-\mathbf{q}')\gamma^\mu u_2(-\mathbf{q})+i\frac{f_v}{2m_N}\overline{u}_2(-\mathbf{q}')\sigma^{\mu\nu}(\mathbf{q}'-\mathbf{q})_\mu u_2(-\mathbf{q})\right)$$

$$=\frac{-1}{(\mathbf{q}'-\mathbf{q})^2+m_v^2}\Big[g_v^2\overline{u}_1(\mathbf{q}')\gamma^\mu u_1(\mathbf{q})(-g_{\mu\nu})\overline{u}_2(-\mathbf{q}')\gamma^\nu u_2(-\mathbf{q})$$

$$-i\frac{f_v g_v}{2m_N}\{\overline{u}_1(\mathbf{q}')\gamma^\mu u_1(\mathbf{q})(-g_{\mu\nu})\overline{u}_2(-\mathbf{q}')\sigma^{\mu\nu}(\mathbf{q}'-\mathbf{q})_\mu u_2(-\mathbf{q})$$

$$+\overline{u}_1(\mathbf{q}')\sigma^{\mu\nu}(\mathbf{q}'-\mathbf{q})_\mu u_1(\mathbf{q})(-g_{\mu\nu})\overline{u}_2(-\mathbf{q}')\gamma^\mu u_2(-\mathbf{q})\}$$

$$-\frac{f_v^2}{4m_\pi^2}\{\overline{u}_1(\mathbf{q}')\sigma^{\mu\nu}(\mathbf{q}'-\mathbf{q})_\mu u_1(\mathbf{q})(-g_{\mu\nu})\overline{u}_2(-\mathbf{q}')\sigma^{\mu\nu}(\mathbf{q}'-\mathbf{q})_\mu u_2(-\mathbf{q})\}\Big] \qquad (2.3.28)$$

Now for the first term of the above equations:

$$\bar{u}_1(\mathbf{q}')\gamma^{\mu}u_1(\mathbf{q})\left(-g_{\mu\nu}\right)\bar{u}_2(-\mathbf{q}')\gamma^{\nu}u_2(-\mathbf{q})$$

$$=\bar{u}_1(\mathbf{q}')\gamma^{0}u_1(\mathbf{q})\left(-g_{00}\right)\bar{u}_2(-\mathbf{q}')\gamma^{0}u_2(-\mathbf{q})+\bar{u}_1(\mathbf{q}')\gamma^{k}u_1(\mathbf{q})\left(-g_{kk}\right)\bar{u}_2(-\mathbf{q}')\gamma^{k}u_2(-\mathbf{q}) \qquad (2.3.29)$$

First we consider the left half of the γ^0 term:

$$\bar{u}_1(\mathbf{q}')\gamma^{0}u_1(\mathbf{q})=\left(1+\frac{\mathbf{q}'\cdot\mathbf{q}+i\sigma_1\cdot(\mathbf{q}'\times\mathbf{q})}{4m_N^2}\right)=\left(1+\frac{\mathbf{p}^2-(1/4)\mathbf{k}^2+i\sigma_1.(\mathbf{k}\times\mathbf{p})}{4m_N^2}\right)$$

[as in the scalar case]

Similarly the right half of the γ^0 term in Eqn. (2.3.29)

$$\bar{u}_2(-\mathbf{q}')\gamma^{0}u_2(-\mathbf{q})=\left(1+\frac{\mathbf{p}^2-(1/4)\mathbf{k}^2+i\sigma_2.(\mathbf{k}\times\mathbf{p})}{4m_N^2}\right)$$

So the γ^0 term in Eqn. (2.3.29) becomes $\left(g^{00}=1\right)$

$$-\left[1+\frac{\mathbf{p}^2}{2m_N^2}-\frac{\mathbf{k}^2}{8m_N^2}+\frac{i}{2m_N^2}\mathbf{S}\cdot(\mathbf{k}\times\mathbf{p})\right] \qquad \text{where } \mathbf{S}=\frac{1}{2}(\sigma_1+\sigma_2).$$

The remaining three terms in Eqn. (2.3.29) for $\gamma^k (k=1,2,3)$ becomes equal to

$$\frac{(E'+m_N)(E+m_N)}{4EE'}\left[\left(\frac{\sigma_1\cdot\mathbf{q}'}{E'+m_N}\sigma_{1x}+\sigma_{1x}\frac{\sigma_1\cdot\mathbf{q}}{E+m_N}\right)\left(\frac{-\sigma_2\cdot\mathbf{q}'}{E'+m_N}\sigma_{2x}+\sigma_{2x}\frac{-\sigma_2\cdot\mathbf{q}}{E+m_N}\right)\right.$$

$$+\left(\frac{\sigma_1\cdot\mathbf{q}'}{E'+m_N}\sigma_{1y}+\sigma_{1y}\frac{\sigma_1\cdot\mathbf{q}}{E+m_N}\right)\left(\frac{-\sigma_2\cdot\mathbf{q}'}{E'+m_N}\sigma_{2y}+\sigma_{2y}\frac{-\sigma_2\cdot\mathbf{q}}{E+m_N}\right)$$

$$\left.+\left(\frac{\sigma_1\cdot\mathbf{q}'}{E'+m_N}\sigma_{1z}+\sigma_{1z}\frac{\sigma_1\cdot\mathbf{q}}{E+m_N}\right)\left(\frac{-\sigma_2\cdot\mathbf{q}'}{E'+m_N}\sigma_{2z}+\sigma_{2z}\frac{-\sigma_2\cdot\mathbf{q}}{E+m_N}\right)\right]$$

where for the left hand part $\bar{u}_1(\mathbf{q}')\gamma^k u_1(\mathbf{q})$, $\gamma^k=\begin{pmatrix}0 & \sigma_1\\ -\sigma_1 & 0\end{pmatrix}$ and for the right hand part

$\bar{u}_2(-\mathbf{q}')\gamma^k u_2(-\mathbf{q})$, $\gamma^k=\begin{pmatrix}0 & \sigma_2\\ -\sigma_2 & 0\end{pmatrix}$ have been used, which after simplifications

becomes $(E\approx E'\approx m_N)$.

$$-\frac{1}{4m_N^2}\left[4\mathbf{p}^2+2i(\sigma_1+\sigma_2)(\mathbf{q}'\times\mathbf{q})-(\sigma_1\ \sigma_2)\mathbf{k}^2+(\sigma_1\cdot\mathbf{k})(\sigma_2\cdot\mathbf{k})\right]$$

Hence the first term of Eqn. (2.3.28) is

$$\frac{g_v^2}{\mathbf{k}^2+m_v^2}\left[1+\frac{3\mathbf{p}^2}{2m_N^2}-\frac{\mathbf{k}^2}{8m_N^2}+i\frac{3}{2m_N^2}\mathbf{S}.(\mathbf{k}\times\mathbf{p})-\frac{1}{4m_N^2}(\boldsymbol{\sigma}_1\cdot\boldsymbol{\sigma}_2)\mathbf{k}^2+\frac{1}{4m_N^2}(\boldsymbol{\sigma}_1\cdot\mathbf{k})(\boldsymbol{\sigma}_2\cdot\mathbf{k})\right] \tag{2.3.30}$$

Considering the non-relativistic reduction $(q'-q)_\mu = i\partial_\mu = i\frac{\partial}{\partial x^\mu}\rightarrow \mathbf{k}$ and $\delta^{\mu\nu}\rightarrow\boldsymbol{\sigma}\times$ together with the non-relativistic Dirac spinors for the last term in Eqn. (2.3.28) we may write

$$\bar{u}_1(\mathbf{q}')\sigma^{\mu\nu}(q'-q)_\mu u_1(\mathbf{q})=-\boldsymbol{\sigma}_1\times\mathbf{k}$$

and $$\bar{u}_2(-\mathbf{q}')\sigma^{\mu\nu}(q'-q)_\mu u_2(-\mathbf{q})=-\boldsymbol{\sigma}_2\times\mathbf{k}$$

So that for the last term, we get

$$-\frac{f_v^2}{4m_N^2}\left[\bar{u}_1(\mathbf{q}')\sigma^{\mu\nu}(\mathbf{q}'-\mathbf{q})_\mu u_1(\mathbf{q})\bar{u}_2(-\mathbf{q}')\sigma^{\mu\nu}(\mathbf{q}'-\mathbf{q})_\mu u_2(-\mathbf{q})\right]$$

$$=-\frac{f_v^2}{4m_N^2}\left[(\boldsymbol{\sigma}_1\ \ \boldsymbol{\sigma}_2)\mathbf{k}^2-(\boldsymbol{\sigma}_1\cdot\mathbf{k})(\boldsymbol{\sigma}_2\cdot\mathbf{k})\right] \tag{2 3.31}$$

In a similar way, considering the non-relativistic approximation for the second term in Eqn. (2.3.28), we obtain

$$\bar{u}_1(\mathbf{q}')\gamma^\mu u_1(\mathbf{q})(-g_{\mu\nu})\bar{u}_2(-\mathbf{q}')\sigma^{\mu\nu}(q'-q)_\mu u_2(-\mathbf{q})+\bar{u}_1(\mathbf{q}')\sigma^{\mu\nu}(q'-q)_\mu u_1(\mathbf{q})(-g_{\mu\nu})\bar{u}_2(-\mathbf{q}')\gamma^\mu u_2(-\mathbf{q})$$

$$=-i\frac{\mathbf{k}^2}{m_N}-\frac{4}{m_N}\mathbf{S}\cdot(\mathbf{k}\times\mathbf{p})-i(\boldsymbol{\sigma}_1\cdot\boldsymbol{\sigma}_2)\frac{\mathbf{k}^2}{m_N}+\frac{i}{m_N}(\boldsymbol{\sigma}_1\cdot\mathbf{k})(\boldsymbol{\sigma}_2\cdot\mathbf{k}) \tag{2.3.32}$$

So, the final result for the whole diagram of one-vector-boson exchange, we obtain the following momentum space potential.

$$V_v(\mathbf{k},\mathbf{p})=\frac{1}{\mathbf{k}^2+m_v^2}\left[g_v^2\left\{1+\frac{3\mathbf{p}^2}{2m_N^2}-\frac{\mathbf{k}^2}{8m_N^2}+\frac{3i}{2m_N^2}\mathbf{S}\cdot(\mathbf{k}\times\mathbf{p})-(\boldsymbol{\sigma}_1\cdot\boldsymbol{\sigma}_2)\frac{\mathbf{k}^2}{4m_N^2}+\frac{1}{4m_N^2}(\boldsymbol{\sigma}_1\cdot\mathbf{k})(\boldsymbol{\sigma}_2\cdot\mathbf{k})\right\}\right.$$
$$+\frac{g_vf_v}{2m_N}\left\{-\frac{\mathbf{k}^2}{m_N}+\frac{4i}{m_N}\mathbf{S}\cdot(\mathbf{k}\times\mathbf{p})-(\boldsymbol{\sigma}_1\cdot\boldsymbol{\sigma}_2)\frac{\mathbf{k}^2}{m_N}+\frac{1}{m_N}(\boldsymbol{\sigma}_1\cdot\mathbf{k})(\boldsymbol{\sigma}_2\cdot\mathbf{k})\right\}$$
$$\left.+\frac{f_v^2}{4m_N^2}\left\{-(\boldsymbol{\sigma}_1\cdot\boldsymbol{\sigma}_2)\mathbf{k}^2+(\boldsymbol{\sigma}_1\cdot\mathbf{k})(\boldsymbol{\sigma}_2\cdot\mathbf{k})\right\}\right] \tag{2.3.32}$$

Going back to the beginning of this section, we notice that with each of the five most important empirical features of the nuclear force (stated in chapter one), one can associate at least one boson field that could provide an explanation. In Table 2.1 we give an overview what each field and coupling predicts for the nuclear force [8].

Table-2.1

Various Meson-Nucleon Couplings and their Contributions to the Nuclear Force as Obtained from One-Boson Exchange

I denotes the isospin of a boson. The characteristics quoted refer to $I = 0$ bosons (no isospin dependence). The isovector ($I = 1$) boson contributions, carrying a factor $\tau_1 \cdot \tau_2$ provide the isospin-dependent forces.

Coupling	Bosons (Strength of Coupling)		Characteristics of predicted forces			
	$I=0$ [1]	$I=1$ $[\tau_1 \cdot \tau_2]$	Central [1]	Spin-Spin $[\sigma_1 \cdot \sigma_2]$	Tensor $[S_{12}]$	Spin-Orbit [L. S]
ps	η (weak)	π (strong)	—	Weak, coherent with *v*	Strong	—
s	σ (strong)	δ (strong)	strong, attractive	—	—	Coherent with *v*
v	ω (strong)	ρ (weak)	strong, repulsive	Weak coherent with *ps*	Opposite to *ps*	Strong, coherent with *s*

The repulsion created by (neutral) vector-boson exchange can be under stood in analogy to the one-photon exchange between like charges creating a repulsive Coulomb potential. Neutral vector bosons can be visualized as heavy photons. The baryon number plays the role of the electric charge. Consequently, in the nucleon-antinucleon system vector-boson exchange generates attraction. The spin-orbit force produced by vector bosons corresponds to the Thomas term, which emerges when the Coulomb potential is employed in the relativistic Dirac Equation. Thus, it can only be understood in a relativistic consideration, the lower component of the Dirac spinor.

We now look into physical manifestations of the fields discussed theoretically so far. In the mass range below the nucleon mass, one finds two pseudoscalar particles, namely π

(138) and η (550), and two vector particles, ρ (769) and ω (783). The (isoscalar) ω has a strong vector coupling and the (isovector) ρ, a strong tensor coupling to the nucleon. Furthermore, there exists an isovector scalar meson, δ (983), which, owing to its large mass and its small coupling constant, provides only a small contribution. Its isospin-dependent central force can be used to adjust the two S waves.

Compared to the (isovector) π, the contribution form the (isosclar) η is very small. This has two reasons: first, the coupling constant of the η is small. Second, the mass of the η is substantially larger than the pion mass. Note that the magnitude of one-meson exchange contributions is roughly proportional to g_α^2/m_α^2, Eqn. (2.1.1) For the reasons given, the η is not so important for the NN system.

Summarizing the important contributions of the mesons discussed so far, the pion as the lightest particle provides the long-range force and, owing to its pseudoscalar nature, the tensor force. This tensor force is reduced at short ranges by the ρ meson to a realistic size. We note that for π and ρ the ps potentials given above have to be multiplied by the operator $\tau_1 \cdot \tau_2$ (with $\frac{1}{2}\tau_i$ the isospin operator for nucleon i), since π and ρ are (isospin one) isovector particles; this factor implies a strong isospin dependence for these two potentials. The ω creates the short-range repulsion and the (short-ranged) spin-orbit force. Thus, these three mesons explain already important features of the nuclear force.

Since there is also strong interaction between pions in relative S wave, there is physical motivation to assume a scalar boson of a mass between 500 and 700 MeV (commonly called σ). Adding this particle to the mesons discussed above defines the so-called one-boson-exchange (OBE) model.

Chapter-3

In-medium NN interaction and Dirac-Brueckner theory

To study the various aspects of the two-nucleon interaction and their influence on nuclear binding energies, one must first have a valid technique for calculating binding energies. The linked-cluster Rayleigh-Schrödinger, or Goldstone expansion, for the ground state energy provides the required technique [6]. To remedy the lack of convergence associated with a hardcore repulsion, Brueckner [10] summed selected terms of this perturbation expansion to define the reaction matrix G. In section one, of this chapter, we derive the Brueckner G-matrix theory in the non-relativistic case where the Pauli-blocking operator for the medium effect has been taken into consideration. A discussion on the effective mass approximation and the angle averaged Pauli operator is given in section two.

Then considering the relativistic approach of G-matrix theory we choose the Thompson equation, which is a relativistic three-dimensional reduction of Bethe-Salpeter equation. There exist many relativistic three-dimensional versions of the Bethe-Salpeter equation, which are all mathematically equally justified. However, some of these equations have unphysical features due to the approximations involved in their derivation. Crucial for our choice of the Thompson equation is the fact that, in the framework of the Thompson equation, meson retardation is ignored i.e. a static meson propagator is used. A reason for ignoring meson retardation is to exclude any false medium effect on meson propagation from the outset. We give the derivation of the Thompson equation in section three. Following the basic philosophy of traditional Brueckner theory, this equation is then applied to nuclear matter in strict analogy to free scattering. This is described in section four, where the solution of Dirac's relativistic equation is used for which the name of this approach is Dirac-Brueckner approach.

3.1 Brueckner Theory and the G-matrix:

To study the influence of various aspects of the two-nucleon interaction on nuclear binding energies, and for calculating the saturation properties, Brueckner [3] suggested the following equation to define the reaction matrix G in the nuclear medium.

$$G(\omega)=V+V\frac{Q}{\omega-h_0}G(\omega) \qquad (3.1.1)$$

The G-matrix plays the role of an effective interaction for two particles in the nuclear medium. It is finite even for singular potentials, in much the same way that the R-matrix for the scattering is finite for singular potentials. In fact, the Eqn.(3.1.1) that defines G, the Brueckner equation, resembles the Lippmann-Schwinger equation for R. The G-matrix differs from the R-matrix for free scattering, by taking into account the Pauli Blocking in the intermediate states as well as the influence of the mean field to nucleons, which appear as single-particle energies in the energy denominator $\omega-h_0$ in Eqn. (3.1.1).

The Hamiltonian h_0 includes a kinetic energy plus a single-particle potential. Acting on product states it gives

$$h_0|\alpha\beta\rangle=(\varepsilon_\alpha+\varepsilon_\beta)|\alpha\beta\rangle \qquad (3.1.2)$$

where the single-particle energies ε_α are simply $\varepsilon_\alpha=\langle\alpha|(p^2/2m_N)+U|\alpha\rangle$. The single-particle potential is itself determined by the interaction of each nucleon with all others in the Fermi sea; for nucleons below the Fermi level it is defined by

$$\langle\mu|U|\mu\rangle=U(k_\mu)=\sum_{\nu<k_F}\langle\mu\nu|G(\varepsilon_\mu+\varepsilon_\nu)|\mu\nu-\nu\mu\rangle, \qquad \text{for } \mu\le k_F \qquad (3.1.3)$$

which includes both direct and exchange terms. The starting energy ω is chosen to be $\omega=\varepsilon_\mu+\varepsilon_\nu$. This definition of U is based on the requirement that U cancels the bubble, or self-energy insertions, that occur on the hole lines in higher-order terms of the Brueckner-Goldstone expansion [32-33]

Once, Eqn. (3.1.1) – (3.1.3) are used to find the G-matrix, the binding energy can be evaluated from

$$E = \sum_{\mu<k_F} \left\langle \mu \left| \frac{p^2}{2m_N} \right| \mu \right\rangle + \frac{1}{2} \sum_{\mu,\nu \le k_F} \left\langle \mu\nu \left| G(\varepsilon_\mu + \varepsilon_\nu) \right| \mu\nu - \nu\mu \right\rangle$$

$$= \sum_{\mu \le k_F} \left(\varepsilon_\mu - \frac{1}{2} U_\mu \right). \tag{3.1.4}$$

Here it is seen that G plays the role of an effective two-body interaction in the nuclear medium. We can now write Eqn. (3.1.1) explicitly by introducing the relative and c.m. momenta $2\mathbf{q}_{\mu\nu} = \mathbf{q}_\mu - \mathbf{q}_\nu$ and $2\mathbf{P}_{\mu\nu} = \mathbf{q}_\mu + \mathbf{q}_\nu$ (We will often omit the state subscripts). The discrete sums now become continuous integrations, i.e. $\sum_\mu \to \Omega(2\pi)^{-3} \int_{k_\mu \le k_F} dk_\mu$.

In our discussion the starting energy, ω, will always be evaluated on the energy shell $\omega \equiv E(\mathbf{q}, \mathbf{P})$ where $E(\mathbf{q}, \mathbf{P})$ is defined in Eqn. (3.1.6). The G-matrix equation is then

$$G(\mathbf{q}', \mathbf{q} \mid \mathbf{P}) = V(\mathbf{q}', \mathbf{q}) - \int \frac{d\mathbf{k} V(\mathbf{q}', \mathbf{k}) Q(\mathbf{k}, \mathbf{P}) G(\mathbf{k}, \mathbf{q} \mid \mathbf{P})}{E(\mathbf{k}, \mathbf{P}) - E(\mathbf{q}, \mathbf{P})} \tag{3.1.5}$$

where $Q(\mathbf{k}, \mathbf{P})$ satisfies the Pauli principle condition given below:

$$Q(\mathbf{k}, \mathbf{P}) = 1 \text{ for } |\mathbf{k} + \mathbf{P}| > k_F$$

$$= 0 \text{ for } |\mathbf{k} \pm \mathbf{P}| \le k_F.$$

In nuclear matter, the single-particle energies are functions of

$$|k_\alpha|, \; \varepsilon(k_\alpha) = (\hbar^2 / 2m_N) k_\alpha^2 + U(|k_\alpha|)$$

Therefore, the above energy denominator is given by

$$E(\mathbf{k}, \mathbf{P}) - E(\mathbf{q}, \mathbf{P}) = \frac{\hbar^2}{m_N} (\mathbf{k}^2 - \mathbf{q}^2) + U(|\mathbf{P} + \mathbf{k}|) + U(|\mathbf{P} - \mathbf{k}|) - U(|\mathbf{P} + \mathbf{q}|) - U(|\mathbf{P} - \mathbf{q}|) \tag{3.1.6}$$

Note that Eqn. (3.1.6) depends on the angles between $\mathbf{P}$ and $\mathbf{k}$, and between $\mathbf{P}$ and $\mathbf{q}$. The Pauli operator $Q(\mathbf{k}, \mathbf{P})$ also depends on the angles between $\mathbf{P}$ and $\mathbf{k}$. The above dependence on angles causes Q to couple states with different relative angular momentum J.

3.2 The effective mass and the angle averaged Pauli operator:

The introduction of the nucleon effective mass is a convenient way to describe the motion of nucleons in the nuclear medium. It reflects the influence of the mean field on the nucleon motion. In the non-relativistic theory, the microscopic mean field $\mathcal{V}_s$ is in general non-local and energy dependent. The effective mass is defined in such a way that it characterizes the energy dependence of a *local* potential V_s which is equivalent to the non-local microscopic potential $\mathcal{V}_s$ [34]:

$$\frac{m_N^*}{m_N} = 1 - \frac{d}{d\varepsilon} V_s(\varepsilon) \tag{3.2.1}$$

The empirical value for the effective mass in nuclear matter derived from the analysis of experimental data in the framework of non-relativistic shell models is

$$\frac{m_N^*}{m_N} \approx 0.7 - 0.8 \tag{3.2.2}$$

In the relativistic treatment of nuclear problems, the concept of "effective mass" is also frequently adopted. However, in this case the term usually denotes different quantities under different circumstance. A quantity that is often referred to as "effective mass" in the relativistic approach is the tilded mass $\tilde{m}_N$, which we introduce in section four of this chapter. This mass is often called the "Dirac mass" [34]. Since its definition has no apparent relation to the non-relativistic definition of the effective mass, Eqn. (3.2.1), the Dirac mass should not be compared to the empirical value of Eqn. (3.2.2) and this wrong comparison should not be considered as a judgment for the relativistic theory itself, or for the underlying bare NN interaction used in the theory.

The angle averaged Pauli operator is used to simplify Eqn. (3.1.5) by eliminating the awkward angle dependence. In the angle average approximation, one replaces the exact Q-operator, $Q(\mathbf{k},\mathbf{P})$, by its average over all angles for fixed $|\mathbf{k}|$ and $|\mathbf{P}|$. The angle averaged Q-operator, $\overline{Q}(\mathbf{k},\mathbf{P})$ is given by [3]

$$\overline{Q}(\mathbf{k},\mathbf{P})=0 \qquad \text{for} \quad k \le \sqrt{k_F^2-P^2}$$

$$=1 \qquad \text{for} \quad k \ge k_F+P$$

$$=\frac{P^2+k^2-k_F^2}{2Pk} \qquad \text{for} \quad \sqrt{k_F^2-P^2}<k\le k_F+P \tag{3.2.3}$$

We note that $\overline{Q}(\mathbf{k},\mathbf{P})$ has discontinuous derivatives at $k=\left(k_F^2-P^2\right)^{1/2}$ and $k=k_F+P$. Using the angle averaged Q-operator, one can eliminate one source of angle dependence. The other remaining dependence on angle is handled by the effective mass approximation. The single-particle energies are assumed to have the quadratic form

$$\varepsilon(k_\alpha)=\frac{\hbar^2k_\alpha^2}{2m_N^*}-U_0 \qquad \text{for } k_\alpha \le k_F$$

$$=\frac{\hbar^2k_\alpha^2}{2m_N} \qquad \text{for } k_\alpha \ge k_F \tag{3.2.4}$$

where m_N^* is called the effective mass. With this choice of single-particle spectrum, the angular dependence disappears from $E(\mathbf{k},\mathbf{P})$ and $E(\mathbf{q},\mathbf{P})$. The resulting expressions are

$$E(\mathbf{k},\mathbf{P})=\frac{\hbar^2}{m_N}\left(\mathbf{P}^2+\mathbf{k}^2\right)=\frac{\hbar^2}{m_N}E_>,$$

$$E(\mathbf{q},\mathbf{P})=\frac{\hbar^2}{m_N^*}\left(\mathbf{P}^2+\mathbf{q}^2\right)-2U_0=\frac{\hbar^2}{m_N}E_<. \tag{3.2.5}$$

The symbols $E_<$ and $E_>$ stand for the energies of two particles below and above the Fermi sea, respectively. We note that the single-particle potential for $q>k_F$ is taken to be zero as previously discussed.

The choice of the hole spectrum, as given by Eqn. (3.2.4) presents a self-consistency problem since Eqn. (3.1.3) relates U and G, the determination of G, however, depends on the choice of U. Therefore, the calculation of U by Eqn. (3.1.3) should reproduce the U used to calculate G. To make U self-consistent in the effective mass approximation, the initial values of m_N^* and U_0 are chosen to calculate G; then from G new values of m_N^* and U_0 are obtained using Eqn. (3.1.3) and Eqn. (3.2.4). This procedure continues until

m_N^* and U_0 change very little; with reasonable starting values for m_N^* and U_0 two or three cycles suffice to achieve self-consistency.

With the angle-averaged $\overline{Q}$ and effective mass approximations, the Brueckner equation Eqn. (3.1.5) becomes

$$G(\mathbf{q}', \mathbf{q} \mid \mathbf{P}) = V(\mathbf{q}', \mathbf{q}) - \int \frac{d\mathbf{k} V(\mathbf{q}', \mathbf{k}) \overline{Q}(\mathbf{k}, \mathbf{P}) G(\mathbf{k}, \mathbf{q} \mid \mathbf{P})}{E(\mathbf{k}, \mathbf{P}) - E(\mathbf{q}, \mathbf{P})} \tag{3.2.6}$$

Neither $\overline{Q}$ nor the energy denominators in Eqn. (3.2.6) now depend on the direction of **P**. Therefore, G is a function of $\mathbf{q}'$, $\mathbf{q}$ and $|\mathbf{P}|$ only.

The calculation of binding energies and self-consistent single-particle energies requires that we solve the Brueckner equation. Even after removal of the above angular dependence, Eqn. (3.2.6) is a three-dimensional integral equation. A partial wave decomposition will be used to reduce Eqn. (3.2.6) to a set of one-dimensional integral equations, just as in the case of the Lippmann-Schwinger equation.

3.3 Thompson equation:

To construct a relativistic theory for the two-nucleon system the Bethe-Salpeter (BS) equation [15] is utilized. The BS equation presents a rather complex mathematical problem when the particles involved are not spin-less and a realistic interaction is employed. In operator notation it may be written as

$$\mathcal{M} = \mathcal{V} + \mathcal{V}\mathcal{G}\mathcal{M} \tag{3.3.1}$$

with $\mathcal{M}$ the invariant amplitude for the two-nucleon scattering process, $\mathcal{V}$ is the sum of all connected two-particle irreducible diagrams, and $\mathcal{G}$ the relativistic two-nucleon propagator. As this four-dimensional integral equation is very difficult to solve, so-called three-dimensional reductions have been proposed, which looks very much like the Lippmann-Schwinger (L.S) equation and which are more amenable to standard methods of numerical solution. The three-dimensional reduction is not unique, and in principle infinitely many choices exist. Typically, they are derived by replacing Eqn. (3.3.1) by two coupled equations:

$$\mathcal{M} = \mathcal{W} + \mathcal{W} g \mathcal{M}, \tag{3.3.2}$$

$$\mathcal{W} = \mathcal{V} + \mathcal{V}(\mathcal{G}-g)\mathcal{W}, \tag{3.3.3}$$

Where g is a covariant three-dimensional propagator with the same elastic unitarity cut as $\mathcal{G}$ in the physical region. In general, the second term on the right hand side of Eqn. (3.3.3) is dropped to arrive at a substantial simplification of the problem. Among the different forms of the three dimensional reductions, the one, suggested by Thompson [35] is particularly suitable for the relativistic many-body problem. Explicitly, we can write BS equation for an arbitrary frame [8]:

$$\mathcal{M}(q', q|P) = \mathcal{V}(q', q|P) + \int d^4k \mathcal{V}(q', k|P)\mathcal{G}(k|P)\mathcal{M}(k, q|P) \tag{3.3.4}$$

with

$$\mathcal{G}(k|P) = \frac{i}{(2\pi)^4} \frac{1}{\left(\frac{1}{2}\not{P} + \not{k} - m_N + i\varepsilon\right)^{(1)}} \times \frac{1}{\left(\frac{1}{2}\not{P} - \not{k} - m_N + i\varepsilon\right)^{(2)}}$$

$$= \frac{i}{(2\pi)^4} \left[\frac{\frac{1}{2}\not{P} + \not{k} + m_N}{\left(\frac{1}{2}P + k\right)^2 - m_N^2 + i\varepsilon}\right]^{(1)} \times \left[\frac{\frac{1}{2}\not{P} - \not{k} + m_N}{\left(\frac{1}{2}P - k\right)^2 - m_N^2 + i\varepsilon}\right]^{(2)} \tag{3.3.5}$$

where q, k and q' are the initial, intermediate and final relative four-momenta, respectively [e.g., $k = (k_0, \mathbf{k})$] and $P = (P_0, \mathrm{P})$ is the total four-momentum; with $\not{P} = \gamma^{\mu} p_{\mu}$ etc. The superscripts refer to particle (1) and (2) and in general, we suppress the spin (or helicity) and isospin indices. Now $\mathcal{G}$ and g have the same discontinuity across the right hand cut, if

$$\mathrm{Im}\,\mathcal{G}(k|P) = -\frac{2\pi^2}{(2\pi)^4}\left(\frac{1}{2}\not{P} + \not{k} + m_N\right)^{(1)}\left(\frac{1}{2}\not{P} - \not{k} + m_N\right)^{(2)}$$

$$\times \delta^{(+)}\left[\left(\frac{1}{2}P + k\right)^2 - m_N^2\right]\delta^{(+)}\left[\left(\frac{1}{2}P - k\right)^2 - m_N^2\right] = \mathrm{Im}\, g(k|P) \tag{3.3.6}$$

with $\delta^{(+)}$ indicating that only the positive-energy root of the argument of the δ function is to be included. From this follows:

$$\mathrm{Im}\, g(k|P) = -\frac{1}{8\pi^2}\left(\frac{1}{2}\not{P} + \not{k} + m_N\right)^{(1)}\left(\frac{1}{2}\not{P} - \not{k} + m_N\right)^{(2)} \frac{\delta\left(\frac{1}{2}P_0 + k_0 - E_{\frac{1}{2}\mathrm{P+k}}\right)\delta\left(\frac{1}{2}P_0 - k_0 - E_{\frac{1}{2}P+k}\right)}{4E_{\frac{1}{2}\mathrm{P+k}}E_{\frac{1}{2}\mathrm{P-k}}} \tag{3.3.7}$$

with $$E_{\frac{1}{2}\mathbf{P}\pm\mathbf{k}} = \left[m_N^2 + \left(\tfrac{1}{2}\mathbf{P}\pm\mathbf{k}\right)^2\right]^{\frac{1}{2}}.$$

Using the equality

$$\delta\left(\tfrac{1}{2}P_0 + k_0 - E_{\frac{1}{2}\mathbf{P}+\mathbf{k}}\right)\delta\left(\tfrac{1}{2}P_0 - k_0 - E_{\frac{1}{2}\mathbf{P}-\mathbf{k}}\right)$$

$$= \delta\left(P_0 - E_{\frac{1}{2}\mathbf{P}+\mathbf{k}} - E_{\frac{1}{2}\mathbf{P}-\mathbf{k}}\right)\delta\left(k_0 - \tfrac{1}{2}E_{\frac{1}{2}\mathbf{P}+\mathbf{k}} + \tfrac{1}{2}E_{\frac{1}{2}\mathbf{P}-\mathbf{k}}\right) \tag{3.3.8}$$

the imaginary part of the propagator $g(k|P)$ can now be written:

$$\operatorname{Im} g(k|P) = -\frac{1}{8\pi^2}\frac{m_N^2}{E_{\frac{1}{2}\mathbf{P}+\mathbf{k}}\,E_{\frac{1}{2}\mathbf{P}-\mathbf{k}}} \times \Lambda_+^{(1)}\left(\tfrac{1}{2}\mathbf{P}+\mathbf{k}\right)\Lambda_+^{(2)}\left(\tfrac{1}{2}\mathbf{P}-\mathbf{k}\right)$$

$$\times\,\delta\left(P_0 - E_{\frac{1}{2}\mathbf{P}+\mathbf{k}} - E_{\frac{1}{2}\mathbf{P}-\mathbf{k}}\right) \times \delta\left(k_0 - \tfrac{1}{2}E_{\frac{1}{2}\mathbf{P}+\mathbf{k}} + \tfrac{1}{2}E_{\frac{1}{2}\mathbf{P}-\mathbf{k}}\right) \tag{3.3.9}$$

where

$$\Lambda_+^{(i)}(\mathbf{p}) = \left[\frac{\gamma^0 E_{\mathbf{p}} - \boldsymbol{\gamma}\cdot\mathbf{p} + m_N}{2m_N}\right]^{(i)} = \sum_{\lambda_i} u(\mathbf{p},\lambda_i)\bar{u}(\mathbf{p},\lambda_i) \tag{3.3.10}$$

represents the positive-energy projection operator for nucleon (i =1, 2) with $u(\mathbf{p})$ a positive-energy Dirac spinor of momentum $\mathbf{p}$; λ_i denotes the helicity or the spin projection of the respective nucleon, and $E_{\mathbf{p}} = \left(m_N^2 + \mathbf{p}^2\right)^{\frac{1}{2}}$.

The projection operators imply that contributions involving virtual anti-nucleon intermediate states are suppressed. These contributions are small when pseudovector coupling is used for the pion. We note that $\operatorname{Im} g(k|P)$ is covariant, since

$$\operatorname{Im} g(k|P) = \operatorname{Im}\mathcal{G}(k|P)$$

Using $\delta(P_0 - E) = 2E\delta(s - E^2 + \mathbf{P}^2)$, where $E = E_{\left(\frac{1}{2}\right)\mathbf{P}+\mathbf{k}} + E_{\left(\frac{1}{2}\right)\mathbf{P}-\mathbf{k}}$

and $s = P^2 = P_0^2 - \mathbf{P}^2$,

Eqn. (3.3.9) can be written as

$$\operatorname{Im} g(k|s) = -\frac{m_N^2}{8\pi^2} \frac{2\left(E_{\frac{1}{2}\mathbf{P}+\mathbf{k}} + E_{\frac{1}{2}\mathbf{P}-\mathbf{k}}\right)}{E_{\frac{1}{2}\mathbf{P}+\mathbf{k}} E_{\frac{1}{2}\mathbf{P}-\mathbf{k}}} \times \Lambda_+^{(1)}\left(\tfrac{1}{2}\mathbf{P}+\mathbf{k}\right)\Lambda_+^{(2)}\left(\tfrac{1}{2}\mathbf{P}-\mathbf{k}\right)$$

$$\times \delta\left(s - \left(E_{\frac{1}{2}\mathbf{P}+\mathbf{k}} + E_{\frac{1}{2}\mathbf{P}-\mathbf{k}}\right)^2 + \mathbf{P}^2\right) \times \delta\left(k_0 - \frac{1}{2}E_{\frac{1}{2}\mathbf{P}+\mathbf{k}} + \frac{1}{2}E_{\frac{1}{2}\mathbf{P}-\mathbf{k}}\right) \tag{3.3.12}$$

Now we try to construct $g(k|s)$ by using a dispersion integral

$$g(k|s) = \frac{1}{\pi} \int_{4m_N^2}^{\infty} \frac{ds'}{s' - s - i\varepsilon} \operatorname{Im} g(k|s') \qquad \left[\text{since } F(w) = \frac{1}{\pi}\int_{-\infty}^{\infty} dw' \frac{\operatorname{Im} F(w')}{w' - w - i\varepsilon}\right] \tag{3.3.13}$$

Inserting Eqn. (3.3 12) in Eqn. (3.3.13) and for the integral in Eqn. (3.313) using the following property of δ function

$$\int dx f(x)\delta[y(x)] = \sum_i \frac{f(x_i)}{|\partial y(x_i)/\partial x|}$$

where x_i are the real roots of $y(x) = 0$ in the interval of integration, we obtain

$$g(k|P) = -\frac{m_N^2}{(2\pi)^3} \frac{2\left[E_{\frac{1}{2}\mathbf{P}+\mathbf{k}} + E_{\frac{1}{2}\mathbf{P}-\mathbf{k}}\right]}{E_{\frac{1}{2}\mathbf{P}+\mathbf{k}} E_{\frac{1}{2}\mathbf{P}-\mathbf{k}}} \times \frac{\Lambda_+^{(1)}\left(\frac{1}{2}\mathbf{P}+\mathbf{k}\right)\Lambda_+^{(2)}\left(\frac{1}{2}\mathbf{P}-\mathbf{k}\right)}{\left(E_{\frac{1}{2}\mathbf{P}+\mathbf{k}} + E_{\frac{1}{2}\mathbf{P}-\mathbf{k}}\right)^2 - P^2 - s - i\varepsilon}$$

$$\times \delta\left(k_0 - \tfrac{1}{2}E_{\frac{1}{2}\mathbf{P}+\mathbf{k}} + \tfrac{1}{2}E_{\frac{1}{2}\mathbf{P}-\mathbf{k}}\right) \tag{3.3.14}$$

This three dimensional propagator is known as the Blankenbecler-Sugar (BbS) choice [18]. By construction, the propagator g has the same discontinuity across the right-hand cut as $\mathcal{G}$; therefore, it preserves the unitary relation satisfied by $\mathcal{M}$.

Using the angle averages $\left(\frac{1}{2}\mathbf{P} \pm \mathbf{k}\right)^2 \approx \frac{1}{4}\mathbf{P}^2 + \mathbf{k}^2$ and $\left(\frac{1}{2}\mathbf{P} \pm \mathbf{q}\right)^2 \approx \frac{1}{4}\mathbf{P}^2 + \mathbf{q}^2$, which should be a very good approximation, Eqn. (3.3.14) assumes the much simpler form

$$g(k|P)=\frac{m_N^2}{(2\pi)^3}\frac{1}{E_{\frac{1}{2}\mathbf{P}+\mathbf{k}}}\times\frac{\Lambda_+^{(1)}\left(\frac{1}{2}\mathbf{P}+\mathbf{k}\right)\Lambda_+^{(2)}\left(\frac{1}{2}\mathbf{P}-\mathbf{k}\right)}{E^2_{\frac{1}{2}\mathbf{P}+\mathbf{q}}-E^2_{\frac{1}{2}\mathbf{P}+\mathbf{k}}+i\varepsilon}\times\delta(k_0) \tag{3.3.15}$$

where we have used $\quad s=4E^2_{\frac{1}{2}\mathbf{P}+\mathbf{k}}-\mathbf{P}^2$

Assuming $\mathcal{W}=\mathcal{V}$, the reduced Bethe-Salpeter equation is obtained in explicit form by replacing in Eqn. (3.3.4) $\mathcal{G}$ by g of Eqn. (3.3.15), yielding

$$\mathcal{M}(\mathbf{q}',\mathbf{q}|\mathbf{P})=\mathcal{V}(\mathbf{q}',\mathbf{q}|\mathbf{P})+\int\frac{d^3k}{(2\pi)^3}\mathcal{V}(\mathbf{q}',\mathbf{k}|\mathbf{P})\frac{m_N^2}{E_{\frac{1}{2}\mathbf{P}+\mathbf{k}}}\frac{\Lambda_+^{(1)}\left(\frac{1}{2}\mathbf{P}+\mathbf{k}\right)\Lambda_+^{(2)}\left(\frac{1}{2}\mathbf{P}-\mathbf{k}\right)}{E^2_{\frac{1}{2}\mathbf{P}+\mathbf{q}}-E^2_{\frac{1}{2}\mathbf{P}+\mathbf{k}}+i\varepsilon}\mathcal{M}(\mathbf{k},\mathbf{q}|\mathbf{P}) \tag{3.3.16}$$

in which both nucleons in the intermediate states are equally far off their mass shell. Taking matrix elements between positive-energy spinors yields an equation for the scattering amplitude in an arbitrary frame:

$$\mathcal{T}(\mathbf{q}',\mathbf{q}|\mathbf{P})=V(\mathbf{q}',\mathbf{q})+\int\frac{d^3k}{(2\pi)^3}V(\mathbf{q}',\mathbf{k})\frac{m_N^2}{E_{\frac{1}{2}\mathbf{P}-\mathbf{k}}}\frac{1}{E^2_{\frac{1}{2}\mathbf{P}-\mathbf{q}}-E^2_{\frac{1}{2}\mathbf{P}+\mathbf{k}}+i\varepsilon}\mathcal{T}(\mathbf{k},\mathbf{q}|\mathbf{P}) \tag{3.3.17}$$

where we have used

$$\begin{aligned}\bar{u}_1\left(\tfrac{1}{2}\mathbf{P}+\mathbf{q}'\right)\bar{u}_2\left(\tfrac{1}{2}\mathbf{P}-\mathbf{q}'\right)\mathcal{V}(\mathbf{q}',\mathbf{q}|\mathbf{P})\,u_1\left(\tfrac{1}{2}\mathbf{P}+\mathbf{q}\right)u_2\left(\tfrac{1}{2}\mathbf{P}-\mathbf{q}\right)&\\ =\bar{u}_1(\mathbf{q}')\,\bar{u}_2(-\mathbf{q}')\,\mathcal{V}(\mathbf{q}',\mathbf{q})\,u_1(\mathbf{q})\,u_2(-\mathbf{q})&\\ \equiv V(\mathbf{q}',\mathbf{q})&\end{aligned} \tag{3.3.18}$$

since this is a Lorentz scalar. An analogous statement applies to $\mathcal{T}$. Calculations of nuclear matter and of finite nuclei are performed in the rest frame of these systems. Thus Eqn. (3.3.17) with the necessary medium modifications would be appropriate for the evaluation of the nuclear matter reaction G-matrix.

In the two-nucleon c.m. frame $\mathbf{P}=0$, so that the BbS propagator $g(\mathbf{k},s)$ reduces to

$$g(\mathbf{k},s)=\frac{1}{(2\pi)^3}\frac{m_N^2}{E_\mathbf{k}}\frac{\Lambda_+^{(1)}(\mathbf{k})\Lambda_+^{(2)}(-\mathbf{k})}{\frac{1}{4}s-E_\mathbf{k}^2+i\varepsilon}\delta(k_0) \tag{3.3.19}$$

which implies the scattering equation

$$\mathcal{T}(\mathbf{q}',\mathbf{q})=V(\mathbf{q}',\mathbf{q})+\int\frac{d^3k}{(2\pi)^3}V(\mathbf{q}',\mathbf{k})\frac{m_N^2}{E_\mathbf{k}}\frac{1}{\mathbf{q}^2-\mathbf{k}^2+i\varepsilon}\mathcal{T}(\mathbf{k},\mathbf{q}) \tag{3.3.20}$$

Two-nucleon scattering is considered most conveniently in the two-nucleon c.m. frame; thus, for calculations of free-space two-nucleon scattering in the BbS approximation, one would use Eqn. (3.3.20).

The BbS propagator is the most widely used approximation. Another choice, which has been frequently applied, is in the version suggested by Thompson. The manifestly covariant form of Thompson's propagator $g(\mathbf{k}, s)$ is the same as Eqn. (3.3.13), but with

$$\int_{4m_N^2}^{\infty} ds'/(s'-s-i\varepsilon) \quad \text{replaced by} \quad \int_{2m_N}^{\infty} d\sqrt{s'}/\left(\sqrt{s'}-\sqrt{s}-i\varepsilon\right).$$

So the Thompson's propagator $g(\mathbf{k}, s)$ now reads

$$g(k|s)=\frac{1}{\pi}\int_{2m_N}^{\infty}\frac{d\sqrt{s'}}{\sqrt{s'}-\sqrt{s}-i\varepsilon}\operatorname{Im} g(k|s')$$

with $\operatorname{Im} g(k|s)$ given in Eqn. (3.3.12).

For the integral in the above equation we again use the same properties of δ-function as in the previous case and obtain [using $f(x)=\dfrac{1}{2\sqrt{s'}\left(\sqrt{s'}-\sqrt{s}-i\varepsilon\right)}$]

$$g(k|P)=-\frac{m_N^2}{(2\pi)^3}\frac{2\left(E_{\frac{1}{2}\mathbf{P}+\mathbf{k}}+E_{\frac{1}{2}\mathbf{P}-\mathbf{k}}\right)}{E_{\frac{1}{2}\mathbf{P}+\mathbf{k}}E_{\frac{1}{2}\mathbf{P}-\mathbf{k}}}\times\frac{\Lambda_+^{(1)}\left(\frac{1}{2}\mathbf{P}+\mathbf{k}\right)\Lambda_+^{(2)}\left(\frac{1}{2}\mathbf{P}-\mathbf{k}\right)}{2\sqrt{\left(E_{\frac{1}{2}\mathbf{P}+\mathbf{k}}+E_{\frac{1}{2}\mathbf{P}-\mathbf{k}}\right)^2-P^2}}$$

$$\frac{1}{\sqrt{\left(E_{\frac{1}{2}\mathbf{P}+\mathbf{k}}+E_{\frac{1}{2}\mathbf{P}-\mathbf{k}}\right)^2-P^2}-\sqrt{s'}-i\varepsilon}\times\delta\left(k_0-\frac{1}{2}E_{\frac{1}{2}\mathbf{P}+\mathbf{k}}+\frac{1}{2}E_{\frac{1}{2}\mathbf{P}-\mathbf{k}}\right)$$

where $$s=4E^2_{\frac{1}{2}\mathbf{P}+\mathbf{k}}-\mathbf{P}^2.$$

Using the angle averages $\left(\frac{1}{2}\mathbf{P}\pm\mathbf{k}\right)^2\approx\frac{1}{4}\mathbf{p}^2+\mathbf{k}^2$ and $\left(\frac{1}{2}\mathbf{P}\pm\mathbf{q}\right)^2\approx\frac{1}{4}\mathbf{p}^2+\mathbf{q}^2$, we obtain

$$g(k|P) = -\frac{m_N^2}{(2\pi)^3}\frac{4E_{\frac{1}{2}\mathbf{P}+\mathbf{k}}}{E^2_{\frac{1}{2}\mathbf{P}+\mathbf{k}}} \times \frac{\Lambda_+^{(1)}\left(\frac{1}{2}\mathbf{P}+\mathbf{k}\right)\Lambda_+^{(2)}\left(\frac{1}{2}\mathbf{P}-\mathbf{k}\right)}{2\sqrt{4E^2_{\frac{1}{2}\mathbf{P}+\mathbf{k}}-P^2}}$$

$$\frac{1}{\sqrt{4E^2_{\frac{1}{2}\mathbf{P}+\mathbf{k}}-P^2}-\sqrt{4E^2_{\frac{1}{2}\mathbf{P}+\mathbf{q}}-P^2}-i\varepsilon} \times \delta(k_0)$$

which after simplification, becomes

$$g(k|P) = \frac{m_N^2}{(2\pi)^3}\frac{1}{E_{\mathbf{k}}E_{\frac{1}{2}\mathbf{P}+\mathbf{k}}} \times \frac{\Lambda_+^{(1)}\left(\frac{1}{2}\mathbf{P}+\mathbf{k}\right)\Lambda_+^{(2)}\left(\frac{1}{2}\mathbf{P}-\mathbf{k}\right)}{2E_{\mathbf{q}}-2E_{\mathbf{k}}+i\varepsilon} \times \delta(k_0) \tag{3.3.21}$$

where $$E_{\frac{1}{2}\mathbf{P}+\mathbf{k}} = \left[\left(\frac{1}{2}\mathbf{P}+\mathbf{k}\right)^2 + m_N^2\right]^{\frac{1}{2}}$$

The equation for the scattering amplitude in an arbitrary frame is then

$$\mathcal{T}(\mathbf{q}',\mathbf{q}|\mathbf{P}) = V(\mathbf{q}',\mathbf{q}) + \int\frac{d^3k}{(2\pi)^3}V(\mathbf{q}',\mathbf{k})\frac{m_N^2}{E_{\mathbf{k}}E_{\frac{1}{2}\mathbf{P}+\mathbf{k}}}\frac{1}{2E_{\mathbf{q}}-2E_{\mathbf{k}}+i\varepsilon}\mathcal{T}(\mathbf{k},\mathbf{q}|\mathbf{P}) \tag{3.3.22}$$

For calculations in the rest frame of nuclear matter or finite nuclei, this equation, together with the necessary medium modifications ($m_N \to \tilde{m}_N$, Pauli projector Q), is appropriate. In our actual calculations in nuclear matter, we replace $E_{\mathbf{k}}$ by $E_{(1/2)\mathbf{P}+\mathbf{k}}$ and $E_{\mathbf{q}}$ by $E_{(1/2)\mathbf{P}+\mathbf{q}}$ in the denominator of Eqn. (3.3.22). This replacement makes possible an interpretation of the energy denominator in terms of differences between single-particle energies, which are typically defined in the rest frame of the many-body system. This allows for a consistent application of this equation in nuclear matter and finite nuclei.

3.4 The relativistic Dirac-Brueckner approach:

The Dirac-Brueckner approach is the outcome of work that was started by Walecka and coworkers for schematic NN interaction. The most advanced relativistic description of nuclear matter has been given by Shakin and coworkers within the frame work of the relativistic Brueckner-Hartree-Fock method [12, 36]. Then after, Horowitz and Serot [37] solved the relativistic Bethe-Goldstone equation and it has been extended to the case of realistic interaction by Machleidt and Brockmann [38].

Similar to conventional Brueckner theory, the basic quantity in the Dirac-Brueckner approach is a $\widetilde{G}$-matrix, which satisfies an integral equation. In this relativistic approach, a relativistic three-dimensional equation is chosen.

We choose the Thompson equation, which is a relativistic three-dimensional reduction of the Bethe-Salpeter equation. Crucial for our choice is the fact that, in the framework of the Thompson equation, meson retardation is ignored (i.e., a static meson propagator is used). This is also true for the Blankenbeckler-Sugar (BbS) equation [18]. We note that in theories, which incorporate meson retardation, effects due to medium modifications on meson propagation in nuclear matter can be calculated. These effects have been investigated by the Bonn group and were found to be small and repulsive. Thus these effects are known and are not very important, for that reason we will ignore them.

When two nucleons scatter from each other in nuclear matter, the medium effects, such as the Pauli blocking for the intermediate states and the density dependence of the nucleon effective mass due to nucleon self-energy, should be taken into account in the Thompson equation describing this process. As in the non-relativistic case, one starts from a bare interaction and carries out a Brueckner calculation to get the effective interaction, often denoted as $\widetilde{G}$ matrix, in the medium.

Following the basic philosophy of traditional Brueckner theory, this equation is applied to nuclear matter in strict analogy to free scattering. Thus including the necessary medium effect, the in-medium Thompson equation, which reads in the nuclear matter rest frame,

$$\widetilde{G}(\mathbf{q}',\mathbf{q}\,|\,\mathbf{P},\widetilde{z})=\widetilde{V}(\mathbf{q}',\mathbf{q})+P\int\frac{d^3k}{(2\pi)^3}\widetilde{V}(\mathbf{q}',\mathbf{k})\frac{\widetilde{m}_N^2}{\widetilde{E}^2_{(1/2)\mathbf{P}+\mathbf{k}}}\frac{\overline{Q}(\mathbf{k},\mathbf{P})}{\widetilde{z}-2\widetilde{E}_{(1/2)\mathbf{P}+\mathbf{k}}}\widetilde{G}(\mathbf{k},\mathbf{q}\,|\,\mathbf{P},\widetilde{z}) \qquad (3.4.1)$$

with $\widetilde{z}=2\widetilde{E}_{(1/2)\mathbf{P}+\mathbf{q}}$ and $\widetilde{m}_N$ the Dirac mass.

$\mathbf{P}$ is the c.m. momentum of the two colliding nucleons in the nuclear medium and q, k, and q' are the initial, intermediate, and final relative momenta, respectively, of the two nucleons interacting in nuclear matter. In Eqn. (3.4.1) we suppressed the k_F dependence as well as spin (helicity) and isospin indices. For $\left|\frac{1}{2}\mathbf{P}\pm\mathbf{q}\right|$ and $\left|\frac{1}{2}\mathbf{P}\pm\mathbf{k}\right|$, the angle average is used.

The relativistic OBE potential to be used in the Dirac-Brueckner calculation is defined as the sum of one-particle-exchange amplitudes of certain bosons with given mass and coupling. Usually six non-strange bosons with mass below 1 GeV are used. The pseudovector (derivative/gradient) coupling, instead of pseudoscalar coupling is used for the pseudoscalar bosons (π and η) in order to avoid un-physically large antiparticle contributions. The details about the derivation of the OBE potential, the parameters (mass, coupling constant, and cutoff of the bosons) and the description of the two-body system have been extensively discussed in chapter 2.

The essential difference between the free-space Thompson equation and the Thompson equation in the medium is the inclusion of the Pauli operator $\overline{Q}(\mathbf{k},\mathbf{P})$ and use of a density dependent effective mass $\tilde{m}_N$, the Dirac mass, in the latter case. The Pauli operator $\overline{Q}(\mathbf{k},\mathbf{P})$ prevents scattering into occupied intermediate states ("Pauli effect"). We note that this is different from Pauli blocking factor for the final states which is always included in the transport models describing nucleus-nucleus collisions. Second, the nucleon mean field due to the medium reduces the mass of the nucleon and affects the energy denominator in Eqn. (3.4.1) which is now density dependent, while in the free Thompson equation the energy denominator uses free relativistic energies ("dispersion effect"). Finally and most importantly, the potential used in the in-medium Thompson equation, as indicated by tilde, is evaluated by using the in-medium Dirac spinors instead of the free ones (hence the name Dirac-Brueckner approach). This leads to the suppression of the attractive σ exchange, which increases with density. The fact that the Dirac-Brueckner approach is able to reproduce quantitatively the saturation properties of nuclear matter is mainly due to this relativistic effect. This observation also implies that the in-medium NN cross sections based on the non-relativistic Brueckner approach lack one important aspect, namely, the effect, which is due to the medium modification of the potential.

The Dirac equation, which is used in this relativistic approach for the description of the single-particle motion in the medium is given by:

$$[\alpha \cdot \mathbf{k} + \beta(\tilde{m}_N + U_S) + U_V]\tilde{u}(\mathbf{k},s) = \varepsilon_k \tilde{u}(\mathbf{k},s) \tag{3.4.2}$$

where U_S is the attractive scalar field and U_V is the time like component of a repulsive vector field; m_N is the mass of free nucleon. The solution of Eqn. (3.4.2) is

$$\tilde{u}(\mathbf{k},s) = \left(\frac{\tilde{E}_k + \tilde{m}_N}{2\tilde{m}_N}\right)^{1/2} \begin{pmatrix} 1 \\ \dfrac{\sigma \cdot \mathbf{k}}{\tilde{E}_k + \tilde{m}_N} \end{pmatrix} \chi_s \tag{3.4.3}$$

with $\tilde{m}_N = m_N + U_S$, $\tilde{E}_k = \left(\tilde{m}_N^2 + \mathbf{k}^2\right)^{1/2}$, σ are the Pauli spin matrices and χ_s is a Pauli spinor. The in-medium Dirac spinor Eqn. (3.4.3) is obtained from free Dirac spinor by replacing m_N by $\tilde{m}_N$. The single particle energy resulting from Eqn. (3.4.2) is given by

$$\varepsilon_k = \tilde{E}_k + U_V \tag{3.4.4}$$

The scalar and vector fields of the Dirac Eqn. (3.4.2) are determined from [8]

$$\frac{\tilde{m}_N}{\tilde{E}_l} U_S + U_V = \sum_{n \le k_F} \frac{\tilde{m}_N^2}{\tilde{E}_m \tilde{E}_n} \left\langle mn \middle| \tilde{G}(\tilde{z}) \middle| mn - nm \right\rangle \tag{3.4.5}$$

which is the relativistic analog to the non-relativistic Brueckner-Hartree-Fock definition of a single-particle potential

$$U(m) = \frac{\tilde{m}_N}{\tilde{E}_m} \langle m | U | m \rangle = \frac{\tilde{m}_N}{\tilde{E}_m} \left\langle m \middle| U_S + \gamma^0 U_V \middle| m \right\rangle = \frac{\tilde{m}_N}{\tilde{E}_m} U_S + U_V \tag{3.4.6}$$

where $|m\rangle$ denotes a state below or above the Fermi surface and corresponds to a continuous choice. The states $|m\rangle$ and $|n\rangle$ are represented by Dirac spinors of the kind in Eqn. (3.4.3) and an appropriate isospin wave function; $\langle m|$ and $\langle n|$ are the adjoint Dirac spinors $\bar{\tilde{u}} = \tilde{u}^\dagger \gamma^0$ with $\bar{\tilde{u}}\tilde{u} = 1$; $\tilde{E}_m = \left(\tilde{m}_N + p_m^2\right)^{1/2}$. The scalar and vector Fields of the Dirac Eqn. (3.4.2) are determined from Eqn. (3.4.5).

The energy per nucleon as a function of the density of the system is often referred to as the nuclear equation of state. We note that this differs from the more common definition of an equation of state, which is the variation of the system pressure with its density.

In the Dirac-Brueckner approach, the nuclear equation of state, that is, the energy per nucleon, ε / A, as a function of density,, ρ, is obtained from the $\widetilde{G}$ matrix :

$$\varepsilon/_{A} = \frac{1}{A} \sum_{m \le k_F} \frac{m_N \widetilde{m}_N + p_m^2}{\widetilde{E}_m} + \frac{1}{2A} \sum_{m,n \le k_F} \frac{\widetilde{m}_N^2}{\widetilde{E}_m \widetilde{E}_n} \left\langle mn \middle| \widetilde{G}(\widetilde{z}) \middle| mn - nm \right\rangle - m_N \qquad (3.4.7)$$

Since the kernel of the in-medium Thompson equation, Eqn. (3.4.1) depends on the solution of the Dirac equation, Eqn. (3.4.2), while for the Dirac equation one needs the scalar and vector potentials which are related to the $\widetilde{G}$ matrix via Eqn. (3.4.4), one has to carry out an iterative procedure with the goal to achieve self-consistency of the two equations: starting from reasonable initial values for $U_s^{(0)}$ and $U_v^{(0)}$, one may solve the in-medium Thompson equation in momentum space by means of the matrix inversion method to get the $\widetilde{G}$ matrix which leads by means of Eqn. (3.4.4) to a new set of values for $U_s^{(1)}$ and $U_v^{(1)}$ to be used in the next iteration; this procedure is continued until convergence is achieved.

Chapter-4

In medium NN scattering cross-section and its density dependence

This chapter is devoted for finding the NN cross-sections in nuclear matter. Since the G-matrix plays the role of an effective interaction for two nucleons in the nuclear medium, we need to find a method suitable for solving the Brueckner G-Matrix equation. In fact, the Brueckner equation that defines G, resembles the Lippmann-Schwinger equation for R matrix. The G-matrix is finite even for singular potentials, in much the same way that the R-matrix for free scattering is finite for singular potentials. As it is true for the R-matrix, one can use the matrix inversion in momentum space to calculate the G-matrix for infinite nuclear matter. In this chapter, we describe the method of matrix inversion for solving the Brueckner G-matrix equation, in section one.

In section 2, we discuss a formula, which can be used to find the NN scattering cross-sections in nuclear medium directly from the G-matrix obtained by solving the Dirac-Brueckner G-matrix equation. The Golden rule for finding the cross-section for the scattering of two free nucleons is derived in section three. This free NN cross-section may be used to find the in-medium NN cross-section by taking into account the Pauli-blocking for the medium effect, which is discussed in the preceding section. In section four, we make an analysis of the effect of the Pauli principle in the binary collisions between the nucleons of a two-nuclear matter system in relative motion. We show that it reduces to a geometrical problem in the momentum space of the system and an analytical derivation for it is presented. Lastly in section five, the lowest-order correction of the density dependence of in-medium nucleon-nucleon cross-sections is obtained from geometrical considerations of the Pauli-blocking effects.

4.1 Matrix inversion method for solving Brueckner equation:

In this section, we first discuss the method of matrix inversion [3] for solving the Schrödinger equation in momentum space. This method can be applied to any non-singular potential, either local or non-local, central or non-central. Several alternate approaches to solve the Schrödinger equation for general non-local potentials are also available in the literature. For the purely nuclear part of the two-nucleon interaction, we find that the direct matrix inversion is simplest.

The Schrödinger equation describing the two-body relative motion is given by

$$\frac{\hbar^2}{m_N}\nabla^2\psi_n(\mathbf{r})+\int d\mathbf{r}V(\mathbf{r}|\mathbf{r}')\psi_n(\mathbf{r})=E_n\psi_n(\mathbf{r}) \tag{4.1.1}$$

where m_N is the nucleon mass, $\mathbf{r}=\mathbf{r}_1-\mathbf{r}_2$ denotes the relative displacement of the two nucleons, and E_n is the total relative energy. In general $V(\mathbf{r}|\mathbf{r}')$ is a non-local operator. For local potentials, $V(\mathbf{r}|\mathbf{r}')\rightarrow\delta(\mathbf{r}-\mathbf{r}')V(\mathbf{r})$; many rapid methods exit for solving the resulting second order differential equation. However, for non-local potentials one faces the difficult task of solving an integro-differential equation in configuration space. Numerical methods for that problem are also available and are particularly useful when Coulomb forces are to be included.

An alternative approach, to be used here for non-local nuclear potentials, is to introduce momentum space. The relative motion is then described by

$$\left(\mathbf{q}'^2-\mathbf{q}^2\right)\psi_n(\mathbf{q}')=\frac{m_N}{\hbar^2}\int d\mathbf{k}\,V(\mathbf{q}'|\mathbf{k})\psi_n(\mathbf{k}) \tag{4.1.2}$$

where $2\mathbf{q}=\mathbf{q}_1-\mathbf{q}_2$ is the relative momentum. The energy eigen-value has been written as $E_n=\frac{\hbar^2\mathbf{q}^2}{m_N}$, where n is used to label the incident momentum vector for scattering and the spin and isospin quantum numbers. The wave function $\psi_n(\mathbf{q}')$ is simply the Fourier transform of $\psi_n(\mathbf{r})$

$$\psi_n(\mathbf{q}')=(2\pi)^{-3/2}\int d\mathbf{r}e^{i\mathbf{q}'\cdot\mathbf{r}}\psi_n(\mathbf{r}) \tag{4.1.3}$$

and the potential matrix elements in momentum space are related to the non-local operator $V(\mathbf{r}|\mathbf{r}')$ by

$$V(\mathbf{q}'|\mathbf{k})=(2\pi)^{-3}\int d\mathbf{r}d\mathbf{r}'e^{-i\mathbf{q}'\cdot\mathbf{r}}V(\mathbf{r}|\mathbf{r}')e^{i\mathbf{k}\cdot\mathbf{r}'}. \tag{4.1.4}$$

The next step is to introduce a partial wave decomposition of the wave function

$$\psi_n(\mathbf{q}')=\sum_{\alpha LL'M} i^{L-L'}\psi^{\alpha}_{LL'}(\mathbf{q}')Y_{LML}(\mathbf{q})\langle LSM_LM_S|JM\rangle y^{JM}_{L'S}(\mathbf{q}')|TT_3\rangle. \tag{4.1.5}$$

The wave function is decomposed into normalized eigenstates of the total angular momentum J, the total spin S, and the total orbital angular momentum L of the two nucleons. Here α denotes the quantum numbers JST. These eigen-states are formed using the Clebsch-Gordon coefficient $\langle LSM_LM_S|JM\rangle$:

$$y^{JM}_{LS}(\mathbf{q}')=\sum_{M_LM_S}\langle LSM_LM_S|JM\rangle Y_{LM_L}(\mathbf{q}')|SM_S\rangle \tag{4.1.6}$$

The corresponding decomposition of the potential is

$$V(\mathbf{q}'|\mathbf{k})=\frac{2}{\pi}\frac{\hbar^2}{m_N}\sum i^{L-L'}V^{\alpha}_{LL'}(\mathbf{q}'|\mathbf{k})y^{JM}_{LS}(\hat{\mathbf{q}}')y^{JM+}_{LS}(\hat{\mathbf{q}}')P_T, \tag{4.1.7}$$

Where $V(\mathbf{q}'|\mathbf{k})$ is an operator in spin and isospin space and P_T is an isospin projection operator. Eqn (4.1.7) represents the most general potential that conserves total angular momentum, parity and isospin. The potential satisfies time reversal invariance if $V_{LL'}(\mathbf{q}'|\mathbf{k})=V_{L'L}(\mathbf{k}|\mathbf{q}')$. The sum is restricted to those quantum numbers $\alpha LL'$ of two-nucleon states that are allowed by the Pauli principle, i.e. states having $S+L+T$ equal to an odd integer For triplet states the orbital angular momenta $L=J\pm1$ can be coupled by a tensor or non-central potential; thus both L and L' labels appear on $V_{LL'}$ and $\psi_{LL'}$.

Let us now consider the scattering problems formulated in momentum space. In momentum space the Schrödinger equation for standing waves is

$$\psi_n(\mathbf{q}')=\delta(\mathbf{q}'-\mathbf{q})|SM_S\rangle|TT_3\rangle-\frac{m_N}{\hbar^2}\frac{\mathrm{P}}{\mathbf{q}'^2-\mathbf{q}^2}\int d\mathbf{k}V(\mathbf{q}'|\mathbf{k})\psi_n(\mathbf{k}) \tag{4.1.8}$$

the symbol P means principal value. The incoming momentum vector $\hbar\mathbf{q}$ and incident spin-isospin state are labeled by n.

Instead of solving directly for the wave function, it is convenient to introduce a reaction matrix defined by $R\phi_n = V\psi_n$, where ϕ_n is a plane wave. The result is the Lippmann-Schwinger equation

$$R(\mathbf{q}'|\mathbf{q}) = V(\mathbf{q}'|\mathbf{q}) - \frac{m_N}{\hbar^2} \mathrm{P} \int \frac{d\mathbf{k} V(\mathbf{q}'|\mathbf{k}) R(\mathbf{k}|\mathbf{q})}{\mathbf{k}^2 - \mathbf{q}^2} \tag{4.1.9}$$

It is easy to construct the wave function and phase shifts from the R-matrix, once a partial wave decomposition is used. The result is the one-dimensional, coupled-channels, Lippmann-Schwinger equation

$$R^{\alpha}_{LL'}(q'|q) = V^{\alpha}_{LL'}(q'|q) - \frac{2}{\pi} \mathrm{P} \sum_{l} \int_{0}^{\infty} \frac{dk\, k^2 V_{Ll}(q'|k) R_{lL'}(k|q)}{k^2 - q^2} \tag{4.1.10}$$

The channels are αL and $\alpha L'$, which can be coupled by a tensor force. In triplet states the orbital angular momenta $L \pm J + 1$ are coupled. For numerical work it is convenient that only real quantities arise in Eqn. (4.1.10). The corresponding wave function in momentum space is

$$\psi^{\alpha}_{LL'}(q') = \frac{1}{q'^2} \delta(q' - q) \delta_{LL'} - \frac{2}{\pi} \mathrm{P} \frac{R_{LL'}(q'|q)}{q'^2 - q^2} \tag{4.1.11}$$

Now we will discuss the way of solving the Lippmann-Schwinger equation for R-matrix. Let us consider Eqn. (4.1.10) for uncoupled channels $(L = L')$ and add a zero term to replace the principal value condition by a smooth integrand

$$R^{\alpha}_{L}(q'|q) = V^{\alpha}_{L}(q'|q) - \frac{2}{\pi} \int_{0}^{\infty} \frac{dk \left[k^2 V^{\alpha}_{L}(q'|k) R^{\alpha}_{L}(k|q) - q^2 V^{\alpha}_{L}(q'|q) R^{\alpha}_{L}(q'|q)\right]}{k^2 - q^2} \tag{4.1.12}$$

The integrand has a finite limit even for $k = q$; however, we wish to avoid such points. We need to solve Eqn. (4.1.12) numerically without having any points at which $k = q$. At the same time we need to find the R-matrix both on and off the energy shell.

These quantities can be easily found by introducing an N-point integration formula

$$\int_{0}^{\infty} dk F(k) = \sum_{j=1}^{N} F(k_j) \omega_j \,, \tag{4.1.13}$$

where we prefer to take k_j and ω_j to be either Laguerre or Gaussian integration points and weights. The integrand in Eqn. (4.1.12) may be considered as $F(k)$ in Eqn. (4.1.13).

Gaussian integration is used for potentials having a relatively slow fall-off in momentum space. All of the N integration points, $k_1, k_2, \ldots\ldots\ldots\ldots, k_N$, are required to be unequal to k_0. If we call k_0 the $N+1$ point $(k_0 \equiv k_{N+1})$, then Eqn.(4.1.12) can be rewritten as

$$V_L^\alpha(k_i|k_{N+1}) = \sum_{j=1}^{N+1} F_L^\alpha(k_i|k_j) R_L^\alpha(k_j|k_{N+1}) \tag{4.1.14}$$

The matrix F_L is simply

$$F_L^\alpha(k_i|k_j) = \delta_{ij} + \omega'_j V_L^\alpha(k_i|k_j) \tag{4.1.15}$$

where ω'_j is defined by

$$\omega'_j = \frac{2}{\pi} \frac{k_j^2 \omega_j}{k_j^2 - k_0^2} \qquad \text{for } j \le N$$

$$= -\frac{2}{\pi} \sum_{m=1}^{N} \frac{\omega_m}{k_m^2 - k_0^2} k_0^2 \qquad \text{for } j = N+1 \tag{4.1.16}$$

The matrix F is nonsingular since k_{N+1} is distinct from the grid points; it can therefore be inverted to yield the R-matrix both on and off the energy shell

$$R^\alpha(k_i|k_{N+1}) = \sum_{j=1}^{N+1} F_L^{-1}(k_i|k_j) V_L^\alpha(k_j|k_{N+1}) \tag{4.1.17}$$

A similar partial wave decomposition may now be used to reduce Brueckner non-relativistic G matrix equation given in Eqn. (3.2.6) to a set of one-dimensional integral equations, just as in the case of the Lippmann-Schwinger equation. To reduce Eqn. (3.2.6) to a set of one-dimensional integral equations, the following standard partial-wave decomposition may be used.

$$G(\mathbf{q}', \mathbf{q}|\mathbf{P}) = \frac{2}{\pi} \cdot \frac{\hbar^2}{m_N} \sum_{\alpha L L' M} i^{L-L'} G_{LL'}^\alpha(\mathbf{q}', \mathbf{q}|\mathbf{P}) \Im_{LS}^{JM}(\hat{\mathbf{q}}') \Im_{L'S}^{JM+}(\hat{\mathbf{q}}) P_T \tag{4.1.18}$$

the resulting one-dimensional coupled-channel non-relativistic Brueckner equation is

$$G_{LL'}^\alpha(q', q|P) = V_{LL'}^\alpha(q', q) - \frac{2}{\pi} \cdot \frac{1}{m_N} \sum_{l} \int_0^\infty \frac{dk\, k^2 \overline{Q}(k,P) V_{LL'}^\alpha(q',k)}{E(k,P) - E(q,P)} \cdot G_{LL'}^\alpha(k, q|P) \tag{4.1.19}$$

In a similar fashion the one-dimensional coupled-channel Dirac-Brueckner relativistic G-matrix equation becomes

$$\widetilde{G}^{\alpha}_{LL'}(q',q|P) = V^{\alpha}_{LL}(q',q) - \frac{2}{\pi}\sum_{l}\int_{0}^{\infty}\frac{dk\,k^2}{(2\pi)^3}\frac{V^{\alpha}_{LL'}(q',k)\widetilde{m}_N}{\widetilde{E}^2_{(1/2)P+k}}\cdot\frac{\overline{Q}(k,P)}{\widetilde{z}-2\widetilde{E}_{(1/2)P+k}}\cdot\widetilde{G}^{\alpha}_{LL'}(k,q|P)$$

(4.1.20)

As before, α denotes JS and T. Eqn. (4.1.20) differs from the Lippmann-Schwinger equation in two important ways. First the energy denominators include single-particle potentials that arise from the presence of the other nucleons – this is simply a recognition of the many-nucleon medium in which the pair is moving. Secondly, the nuclear medium produces the Pauli exclusion effect as recorded in $\overline{Q}$. Because of $\overline{Q}$, the integrand in Eqn. (4.1.20) does not have a singularity, which causes the healing of the two-nucleon wave function in the nuclear medium.

The nonsingular character of the integrand of Eqn. (4.1.20) makes it completely suitable to solve by matrix inversion method.

4.2 Effective cross-sections for NN elastic scattering:

In this section we consider nucleon energies below the pion threshold (~300 MeV), so that the NN scattering is purely elastic. When discussing two-body properties in nuclear matter, we shall use the concept of *effective cross sections* [39]. In the following discussion, four different cross section values are distinguished. The free NN cross section, which in our approach is related to the vacuum t matrix T_{11}, will be called σ_4. In some kinetic equations, this cross section is corrected for Pauli blocking in the outgoing channel. We shall call this value σ_3. Calculating the effective cross-section from the effective Dirac-Brueckner interaction, $\widetilde{G}$, we obtain σ_1 and σ_2. Here, σ_2 is not corrected for Pauli blocking in the outgoing channel (but Pauli-blocking in the intermediate NN channels is included); σ_1 is the effective cross-section that contains all medium corrections. The incoming NN channel is the same for all four cross sections. Particle 1 has a certain fixed momentum compared to the surrounding nuclear medium. For particle 2, all the available Fermi sea momenta are taken into account and averaged afterward. In summary [39], (writing σ for σ_1)

$$\sigma(q_1)=\frac{3}{4\pi^2 k_F^3}\int_0^{k_F} d^3q_2\overline{Q}(P,s^*,q)\frac{\widetilde{m}_N^4(\hbar c)^2}{2(2\pi)^2 s^*}\times\int d\Omega_{c.m.}\sum_{\sigma,\tau}\left|\widetilde{G}(\mathbf{q}',\mathbf{q}|\mathbf{P})\right|^2 \qquad (4.2.1)$$

where $\mathbf{q}_1$ and $\mathbf{q}_2$ stands for momentum of particle 1 and 2 respectively, $\mathbf{P}=\mathbf{q}_1+\mathbf{q}_2$, $s^*=\left(\widetilde{E}_1+\widetilde{E}_2\right)^2-\mathbf{P}^2$ and $P=\frac{1}{2}\sqrt{s^*-4\widetilde{m}_N^2}$ and $\sum_{\sigma,\tau}$ represents the summation (average) of outgoing (incoming) spin and isospin channels. The function $\overline{Q}$ gives the angle-averaged Pauli-blocking operator and k_F denotes the Fermi momentum.

The starting energy in Eqn. (3.4.1) is $\widetilde{z}=2\widetilde{E}_{\mathbf{q}}=2\sqrt{\widetilde{m}_N^2+\mathbf{q}^2}$, where q is related to the kinetic energy of the incident nucleon in the "laboratory system" (E_{lab}), by $E_{lab}=2q^2/m_N$ in which the other nucleon is at rest. Here two colliding nucleons are considered in nuclear matter. The Pauli projector is represented by one Fermi sphere as in conventional nuclear matter calculations This Pauli projector, which is originally defined in the nuclear matter rest frame, must be boosted to the c.m. frame of the two interacting nucleons. The explicit formulae for $\overline{Q}$ [40] is as follows:

$$\overline{Q}(q,P,s^*)=0 \qquad \text{for } q\le\frac{1}{\gamma}\left\{\gamma^2k_F^2-\left(\eta\widetilde{E}_F\right)^2\right\}^{1/2}$$

$$\overline{Q}(q,P,s^*)=1 \qquad \text{for } q\ge\eta\widetilde{E}_F+\gamma\, k_F$$

$$\overline{Q}(q,P,s^*)=\left\{\frac{-2\eta\widetilde{E}_F}{\gamma^2}+\left[\left(\frac{2\eta\widetilde{E}_F}{\gamma^2}\right)^2+4\left(1-\frac{1}{\gamma^2}\right)\left(\frac{\eta^2\widetilde{E}_F^2}{\gamma^2}+q^2-k_F^2\right)\right]^{1/2}\right\}\left\{2q\left(1-\frac{1}{\gamma^2}\right)\right\}^{-1}$$

$$\text{for other values of } q, \qquad (4.2.2)$$

with $\widetilde{E}_F=\left\{k_F^2+\widetilde{m}_N^2\right\}^{1/2}$ and furthermore η and γ are defined by:

$$\eta=P/\sqrt{s^*} \text{ and } \gamma=\widetilde{E}/\sqrt{s^*}=\sqrt{s^*+P^2}/\sqrt{s^*}.$$

In c.m. frame $\eta=0$ and $\gamma=1$, so that $\overline{Q}$ takes the form

$$\overline{Q}(q,P,s^*)=0 \qquad \text{for } q\le k_F$$

$$\overline{Q}(q,P,s^*)=1 \qquad \text{for } q\ge k_F \qquad (4.2.3)$$

For in-medium NN scattering, the Dirac-Brueckner $\widetilde{G}$-matrix of Eqn. (3.4.1) may be used in Eqn. (4.2.1) in center of mass frame with $\mathbf{P}=0$ and $\widetilde{z}=2\widetilde{E}_q$. We may obtain this

$\widetilde{G}$-matrix by solving the Dirac-Brueckner $\widetilde{G}$-matrix equation using the matrix inversion method, discussed in the previous section. Thus the in-medium NN cross-sections may be calculated directly from the Dirac-Brueckner $\widetilde{G}$-matrix by using the cross-section formula given in Eqn. (4.2.1).

4.3 The Golden rule for free NN cross-section:

In this section we begin a quantitative formulation of elementary particle dynamics, which amounts, in practice, to calculation of scattering cross sections (σ). The procedure involves two distinct parts (1) evaluation of the relevant Feynman diagrams to determine the "amplitude" $(\mathcal{M})$ for the process in question, and (2) insertion of $\mathcal{M}$ into Fermi's 'Golden Rule" to compute σ.

Now the question is what we mean by a "cross section". Suppose a particle (may be an electron) comes along, encounters some kind of potential, and scatters off at an angle θ. This *scattering angle* is a function of the *impact parameter b*, the distance by which the incident particle would have missed the scattering center, had it continued on its original trajectory. Ordinarily, the smaller impact parameter, the larger the deflection, but the actual functional form of $\theta(b)$ depends on the particular potential involved.

If the particle comes in with an impact parameter between b and $b+db$, it will emerge with a scattering angle between θ and $d\theta$. More generally, if it passes through an infinitesimal *area* $d\sigma$, it will scatter into a corresponding *solid angle* $d\Omega$. Naturally, the larger we make $d\sigma$, the larger $d\Omega$ will be. The proportionality factor is called the *differential scattering cross section, D*;

$$d\sigma = D(\theta)d\Omega$$

In principle, D might depend on the azimuthal angle ϕ; however, most potentials of interest are spherically symmetrical, in which case the differential cross section depends only on θ. By the way, the notation, D, is simply $d\sigma/d\Omega$.

Suppose now, that we have a *beam* of incoming particles, with uniform *luminosity* $\mathcal{L}$ ($\mathcal{L}$ is the number of particles per unit time, per unit area). Then $dN = \mathcal{L}d\sigma$ is the number of particles per unit time passing through area $d\sigma$, and hence also the number per unit time scattered into solid angle $d\Omega$:

$$dN = \mathcal{L}d\sigma = \mathcal{L}\,D(\theta)d\Omega$$

It follows that

$$\frac{d\sigma}{d\Omega} = D(\theta) = \frac{1}{\mathcal{L}}\frac{dN}{d\Omega}$$

This is frequently a more convenient way to think of the differential cross section. It is the number of particles per unit time scattered into solid angle $d\Omega$, divided by $d\Omega$ and by the luminosity.

To calculate the basic physical quantity scattering cross section there are two ingredients: (1) the *amplitude* $(\mathcal{M})$ for the process and (2) the *phase space* available. The amplitude contains all the *dynamical* information; we calculate it by evaluating the relevant Feynman diagrams, using the "Feynman rules" appropriate to the interaction in question. The phase space factor contains only *kinematical* information; it depends on the masses, energies, and momenta of the participants.

Suppose that the particles 1 and 2 have a collision, producing particles 3,4,.........,n so that

$$1 + 2 \rightarrow 3 + 4 + \ldots\ldots\ldots + n \qquad (4.3.1)$$

The cross section is given by the formula known as the Golden rule [29]:

$$d\sigma = |\mathcal{M}|^2 \frac{\hbar^2 S}{4\sqrt{(q_1 \cdot q_2)^2 - (m_1 m_2 c^2)^2}}\left[\left(\frac{c d^3\mathbf{q}_3}{(2\pi)^3 2E_3}\right)\left(\frac{c d^3\mathbf{q}_4}{(2\pi)^3 2E_4}\right)\cdots\cdots\left(\frac{c d^3\mathbf{q}_n}{(2\pi)^3 2E_n}\right)\right]$$

$$\times (2\pi)^4 \delta^4(q_1 + q_2 - q_3 - q_4 - \ldots\ldots\ldots\ldots - q_n) \qquad (4.3.2)$$

where $q_i = (E_i / c, \mathbf{q}_i)$ is the four-momentum of the i-th particle which carries mass m_i, $E_i^2 - \mathbf{q}_i^2 c^2 = m_i^2 c^4$, and S is a statistical factor ($1/j!$) for each group of j identical particles in the final state). $(\mathcal{M})$ is the scattering amplitude. The delta function enforces conservation of energy and momentum.

The above equation determines the cross section for a process in which the three-momentum of particle 3 lies in the range $d^3\mathbf{q}_3$ about the value $\mathbf{q}_3$, that of particle 4 falls in the range $d^3\mathbf{q}_4$ about $\mathbf{q}_4$, and so on. In a typical situation we study only the angle at which particle 3 emerges. In that case we integrate over all the other momenta $(\mathbf{q}_4, \mathbf{q}_5, \ldots\ldots\ldots\ldots, \mathbf{q}_n)$, and over the magnitude of $\mathbf{q}_3$; what's left gives us $d\sigma/d\Omega$, the differential cross section for the scattering of particle 3 into solid angle $d\Omega$.

Let us now consider two-body scattering where $1+2 \rightarrow 3+4$. Here

$$d\sigma = |\mathcal{M}|^2 \frac{\hbar^2 S}{4\sqrt{(q_1.q_2)^2-(m_1 m_2 c^2)^2}}\left[\frac{c d^3\mathbf{q}_3}{(2\pi)^3 2E_3}\frac{c d^3\mathbf{q}_4}{(2\pi)^3 2E_4}\right]\times(2\pi)^4\delta^4(q_1+q_2-q_3-q_4)$$

$$=\left(\frac{\hbar c}{8\pi}\right)^2 \frac{S|\mathcal{M}|^2}{\sqrt{(q_1.q_2)^2-(m_1 m_2 c^2)^2}}\frac{d^3\mathbf{q}_3 d^3\mathbf{q}_4}{E_3 E_4}\delta^4(q_1+q_2-q_3-q_4) \qquad (4.3.3)$$

Now since $(q_1.q_2)^2 = \left(\frac{E_1 E_2}{c^2} - \mathbf{q}_1\cdot\mathbf{q}_2\right)^2$, we write

$$\sqrt{(q_1.q_2)^2-(m_1 m_2 c^2)^2} = \frac{(\mathbf{q}_1 E_2 - \mathbf{q}_2 E_1)}{c} \qquad (4.3.4)$$

Rewriting the delta function as

$$\delta^4(q_1+q_2-q_3-q_4) = \delta\left(\frac{E_1+E_2-E_3-E_4}{c}\right)\delta^3(\mathbf{q}_1+\mathbf{q}_2-\mathbf{q}_3-\mathbf{q}_4)$$

and expressing the outgoing energies in terms of $\mathbf{q}_3$ and $\mathbf{q}_4$ i.e.

$E_3 = c\sqrt{m_3^2 c^2 + \mathbf{q}_3^2}$, $\quad E_4 = c\sqrt{m_4^2 c^2 + \mathbf{q}_4^2}$, we get

$$d\sigma = \left(\frac{\hbar c}{8\pi}\right)^2 \frac{S|\mathcal{M}|^2 c}{(\mathbf{q}_1 E_2 - \mathbf{q}_2 E_1)}\frac{d^3\mathbf{q}_3 d^3\mathbf{q}_4}{E_3 E_4}\delta\left(\frac{E_1+E_2-E_3-E_4}{c}\right)\delta^3(\mathbf{q}_1+\mathbf{q}_2-\mathbf{q}_3-\mathbf{q}_4).$$

performing the $\mathbf{q}_4$ integral, we obtain

$$d\sigma = \left(\frac{\hbar}{8\pi}\right)^2 \frac{S|\mathcal{M}|^2 c}{(\mathbf{q}_1 E_2 - \mathbf{q}_2 E_1)}\frac{\delta\left[(E_1+E_2)/c - \sqrt{m_3^2c^2+\mathbf{q}_3^2} - \sqrt{m_4^2c^2+(\mathbf{q}_1+\mathbf{q}_2-\mathbf{q}_3)}\right]}{\sqrt{m_3^2c^2+\mathbf{q}_3^2}\sqrt{m_4^2c^2+(\mathbf{q}_1+\mathbf{q}_2-\mathbf{q}_3)}}d^3\mathbf{q}_3$$

(4.3.5)

Writing $d^3\mathbf{q}_3 = \rho^2 d\rho\, d\Omega$ (where ρ is shorthand for $|\mathbf{q}_3|$ and $d\Omega = \sin\theta\, d\theta\, d\phi$) we get

$$\frac{d\sigma}{d\Omega}=\left(\frac{\hbar}{8\pi}\right)^2\frac{Sc}{(\mathbf{q}_1E_2-\mathbf{q}_2E_1)}\int_0^\infty|\mathcal{M}|^2\frac{\delta\left[(E_1+E_2)/c-\sqrt{m_3^2c^2+\rho^2}-\sqrt{m_4^2c^2+(\mathbf{q}_1+\mathbf{q}_2-\rho)^2}\right]}{\sqrt{m_3^2c^2+\rho^2}\sqrt{m_4^2c^2+(\mathbf{q}_1+\mathbf{q}_2-\rho)^2}}\rho^2d\rho \tag{4.3.6}$$

Let

$$E\equiv c\left(\sqrt{m_3^2c^2+\rho^2}+\sqrt{m_4^2c^2+(\mathbf{q}_1+\mathbf{q}_2-\rho)^2}\right)$$

So, equation (4.3.6) becomes

$$\frac{d\sigma}{d\Omega}=\left(\frac{\hbar}{8\pi}\right)^2\frac{Sc}{(\mathbf{q}_1E_2-\mathbf{q}_2E_1)}\int_0^\infty|\mathcal{M}|^2\frac{\rho^2}{\rho E-c(\mathbf{p}_1+\mathbf{p}_2)\sqrt{m_3^2c^2+\rho^2}}\delta[(E_1+E_2)/c-E/c]dE$$

$$=\left(\frac{\hbar c}{8\pi}\right)^2\frac{S}{(\mathbf{q}_1E_2-\mathbf{q}_2E_1)}\int_0^\infty|\mathcal{M}|^2\times\frac{|\mathbf{q}_3|^2}{|\mathbf{q}_3|(E_1+E_2)-c(\mathbf{q}_1+\mathbf{q}_2)\sqrt{m_3^2c^2+|\mathbf{q}_3|^2}} \tag{4.3.7}$$

In the centre of mass frame $\mathbf{q}_1=-\mathbf{q}_2$, $|\mathbf{q}_1|=|\mathbf{q}_2|$. So that equation (4.3.7) becomes

$$\therefore\frac{d\sigma}{d\Omega}=\left(\frac{\hbar c}{8\pi}\right)^2\frac{S|\mathcal{M}|^2}{(E_1+E_2)^2}\frac{|\mathbf{q}_f|}{|\mathbf{q}_i|} \tag{4.3.8}$$

where $|\mathbf{q}_f|$ is the magnitude of either outgoing momentum and $|\mathbf{q}_i|$ is the magnitude of either incoming momentum.

4.4 Geometrical consideration of the Pauli-blocking effect of the medium on NN cross-section

The in-medium NN cross-sections may also be determined from the free NN cross-section. The main effect of the medium corrections is due to Pauli-blocking of nucleon-nucleon scattering. Pauli-blocking prevents the nucleons from scattering into final occupied states in binary collisions between the projectile and target nucleons.

The effect of Pauli-blocking for the in-medium in nucleon-nucleus collisions was first investigated by Goldberger in 1948 and by Clementel and Villi in 1955 on the basis of the geometry for a single nucleon-nucleon collision in momentum space. Their approach is still used in the microscopic descriptions of nucleon-nucleus cross-section with good agreement with the experimental data [41]. We will see how one can extend their ideas to the study of the collision between two nucleons in the nuclear matter.

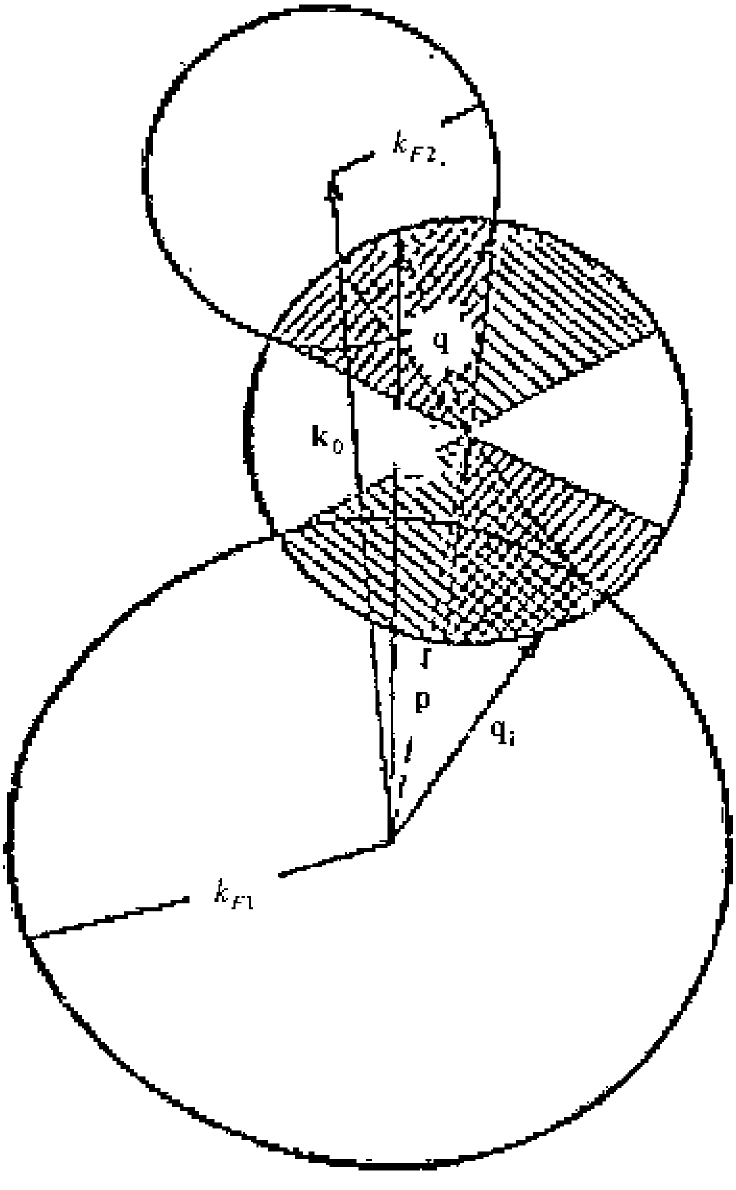

Fig. 4.1: Diagram exhibiting the kinematics of the two nucleon collision. The initial momenta of the pair, $\mathbf{q}_1$ and $\mathbf{q}_2$, together with $\mathbf{k}_0$, $\mathbf{p}$ and $\mathbf{q}$ are represented by arrows as indicated. The third sphere is the locus of the end points of the vector $\mathbf{q}$. The non-shaded region corresponds to the allowed scattering angle. The cross-hatched region indicates the admissible angles for initial pairs with the same modulus $2p$ for the total momentum and the same modulus $2q$ for the relative momentum.

By nuclear matter collisions we mean two Fermi fluids, one of which is initially at rest and the other is moving against the first with a momentum $\mathbf{k}_{lab} = \mathbf{k}_0$ per nucleon. Each of these fluids possesses a Fermi motion in its rest frame and the initial state of the system is described by two filled spheres of radii k_{F1} and k_{F2}, corresponding respectively to the larger and smaller spheres, with the position of their centers separated by k_0, as shown in Fig. 4.1. In the initial stage of the system a binary collision between a pair of nucleons will only be possible if they pertain to different Fermi fluids. If initially they have momenta $\mathbf{q}_1$ and $\mathbf{q}_2$, after the collision they will possess momenta $\mathbf{q}_1'$ and $\mathbf{q}_2'$, which by the Pauli principle must lie outside both Fermi spheres. These momenta are also related by the energy-momentum conservation laws

$$\mathbf{q}_1 + \mathbf{q}_2 = \mathbf{q}_1' + \mathbf{q}_2'$$
$$\mathbf{q}_1' - \mathbf{q}_2' = \hat{\varepsilon}\left|\mathbf{q}_1 - \mathbf{q}_2\right| \tag{4.4.1}$$

where $\hat{\varepsilon}$ is a unit vector in the direction of a solid angle $d\Omega$. We observe that the conservation of energy of relative motion in the binary collision is only valid for energies below the pion-threshold $E_{lab} \approx 300$ MeV above which most of the collision cross section will be inelastic due to pion production. Nevertheless, we shall see that for relative motion energy of the Fermi fluids greater than this value, the Pauli principle has a rapidly decreasing importance and the above assumption can be used without major consequences.

In Fig. 4.1 we observe that, due to Pauli principle and the conservation laws in Eqn. (4.4.1), the available solid angle $4\pi\omega_S$ denoted by Ω_{Pauli}, the Pauli-blocking for scattering of the pair is restricted to the non-hatched region inside the auxiliary sphere of radius $q = \left|\mathbf{q}_1 - \mathbf{q}_2\right|/2$. To this solid angle not only a pair but all pairs of nucleons can scatter which lie on the surface of this auxiliary sphere and inside the double-hatched region of Fig. 4.1. This double-hatched region forms a solid angle $4\pi\omega_I$. The calculation of ω_S and ω_I is of great relevance in our following analysis and we show that it can be translated into a problem of spherical geometry. We see that energy and momentum conservation, together with the Pauli principle, restrict the collision phase space to a complex geometry involving the Fermi-spheres and the scattering sphere. In this scenario, the in-medium cross-section corrected by Pauli-blocking can be defined as [42]

$$\sigma_{NN}(k_0, k_{F1}, k_{F2}) = \int \frac{d^3k_1 d^3k_2}{(4\pi k_{F1}^3/3)(4\pi k_{F2}^3/3)} \frac{2q}{k_0} \sigma_{NN}^{free}(q) \frac{\Omega_{Pauli}}{4\pi} \tag{4.4.2}$$

where k_0 is the relative momentum per nucleon of the nucleus-nucleus collision and $\sigma_{NN}^{free}(q)$ is the free nucleon-nucleon cross-section for the relative momentum $2\mathbf{q} = \mathbf{q}_2 - \mathbf{q}_1$ of a given pair of colliding nucleons and the integrations are carried out inside different Fermi spheres The factor $\frac{\Omega_{Pauli}}{4\pi}$ is the fraction of the solid angle available for a specific collision between a nucleon with momentum $\mathbf{q}_1$ and another with momentum $\mathbf{q}_2$. The factor $\frac{2q}{k_0}$ corrects for the flux differences between the laboratory system and a system in which one of the nucleons is at rest. Now we define

$$\mathbf{p} = \frac{\mathbf{q}_1 + \mathbf{q}_2}{2}$$

$$\mathbf{q} = \frac{\mathbf{q}_2 - \mathbf{q}_1}{2} \tag{4.4.3}$$

$$\text{and} \quad \mathbf{b} = \mathbf{k}_0 - \mathbf{p}$$

After the collision $\mathbf{p}$ and $\mathbf{b}$ stay constant while $\mathbf{q}$ changes only its direction.

Fig. 4.1 shows schematically the geometry of the collision. The allowed scattering angle of the pair corresponds to the non-hatched region of the spherical surface with center in $\mathbf{p}$ and radius equal to q. This angle is equal to $4\pi\omega_S = \Omega_{Pauli}$, according to the definition. The possible angle of origin of nucleon–pairs with the same momentum $\mathbf{p}$ and same modulus q of the relative momentum is given by the double-hatched region in Fig.4.1. We call this angle $2\overline{\Omega}$ and we note that it corresponds to $4\pi\omega_I$ according to the definition. This solid angle is geometrically originated by the intersection of two hour glass-shaped angle each of which is single-hatched in Fig.4.1 and which we call $2\Omega_a$ and

$2\Omega_b$. These angles are easily related to the momenta defined in Eqn. (4.4.3). This can be verified in Fig.4.1 from which we infer that

$$\Omega_a = 2\pi(1-\cos\theta_a)$$
$$\Omega_b = 2\pi(1-\cos\theta_b) \tag{4.4.4}$$

where

$$\cos\theta_a = \frac{p^2+q^2-k_{F1}^2}{2pq}$$

and

$$\cos\theta_b = \frac{b^2+q^2-k_{F2}^2}{2bq} \tag{4.4.5}$$

we then immediately have that

$$\Omega_{Pauli} = 4\pi\,\omega_S = 4\pi - 2\left(\Omega_a+\Omega_b-\overline{\Omega}\right) \quad \text{where } 4\pi\,\omega_I = 2\overline{\Omega} \tag{4.4.6}$$

Using Eqn. (4.4.4) in the above equation, we obtain

$$\Omega_{Pauli} = 4\pi(\cos\theta_a+\cos\theta_b-1)+2\overline{\Omega} \tag{4.4.7}$$

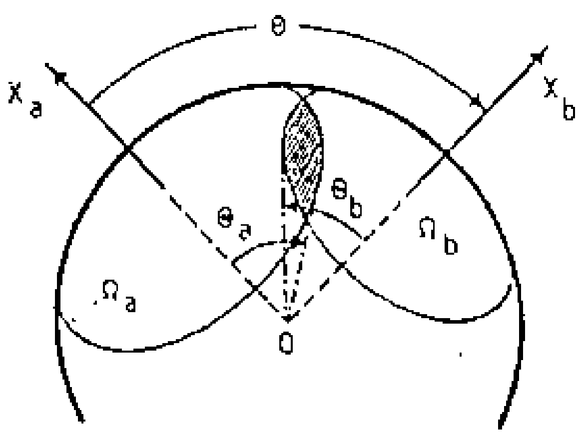

Fig. 4.2: Spherical surface of unit radius over which we traced two circles originated by its intersection with the solid angels Ω_a and Ω_b. The solid angle $\Omega_a(\Omega_b)$ possesses a symmetry angle $\theta_a(\theta_b)$ with respect to the axis $X_a(X_b)$. These axes have an angle θ between them. The shaded area is simultaneously inside Ω_a and Ω_b.

The angle $\overline{\Omega}$ depends on θ_a, θ_b and on the angle θ between $\mathbf{b}$ and $\mathbf{p}$. This situation is shown more clearly in Fig.4.2 where the axes X_a and X_b are respectively parallel to $\mathbf{p}$

and b. The solid angles Ω_a, Ω_b and $\overline{\Omega}$ are now given by the corresponding areas inscribed over the surface of a sphere of unit radius. It is clear from this figure that

$$\begin{aligned} &\text{i)} \quad \overline{\Omega}=\Omega_b && \text{if } \theta \leq \theta_a - \theta_b \geq 0 \\ &\text{ii)} \quad \overline{\Omega}=\Omega_a && \text{if } \theta \leq \theta_b - \theta_a \geq 0 \\ &\text{iii)} \quad \overline{\Omega}=0 && \text{if } \theta \geq \theta_a + \theta_b \end{aligned} \tag{4.4.8}$$

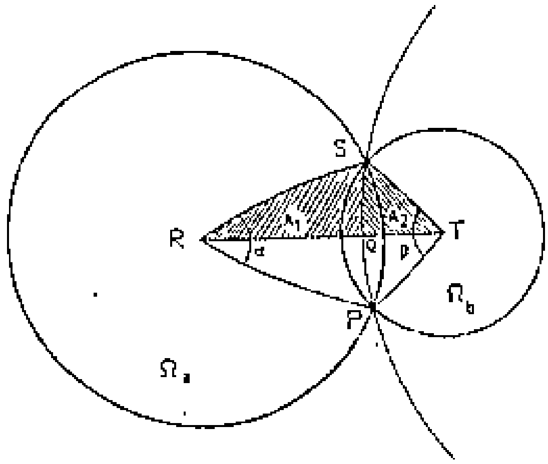

Fig.4.3: The projection into a plane of the area Ω_a and Ω_b. R and T are their geometrical centers. S and P are the intersection points of their contours. All lines joining these points are segments of great circles over the spherical surface. A_1 and A_2 are the areas of two spherical triangles limited by some of these lines.

The case $|\theta_a - \theta_b| \leq \theta \leq \theta_a + \theta_b$, as it appears in Fig.4.3 needs a more detailed study. In Fig.4.3, R and T are the centers of these circular areas, S and P are the intersection-points of the circular contours of these areas and Q is the point where the geodesic line joining R and T crosses the geodesic line joining S and P. The points R, P and S define a spherical triangle of area $2A_1$. The points S, P and T define a spherical triangle of area $2A_2$. These triangles have internal angles α and β around R and T, respectively.

The part of the circular area Ω_a, which is inside the lines RS and RP is equal to $\frac{\alpha}{2\pi}\Omega_a$.
The part of the circular area Ω_b, which is inside the lines TS and TP is equal to $\frac{\beta}{2\pi}\Omega_b$.
We then easily deduce from Fig. 4.3 that the intersection area between Ω_a and Ω_b is

$$\overline{\Omega}=\frac{\alpha}{2\pi}\Omega_a+\frac{\beta}{2\pi}\Omega_b-2A_1-2A_2 \tag{4.4.9}$$

To obtain the angle α we use two new axes X_P and X_S passing by the center of the spherical surface and by the points P and S, respectively. Adopting a polar coordinate system in which X_a is the z-axis, the angle will be the difference between the azimuthal angles between X_P and X_S. In this coordinate system (θ_a,ϕ_P) and (θ,ϕ_b) are the polar and azimuthal angles corresponding to the axes X_P and X_b, respectively. Since the angle between X_b and X_P is θ_b, then

$$\cos\theta_b=\cos\theta_a\cos\theta+\sin\theta_a\sin\theta\cos(\phi_b-\phi_P) \tag{4.4.10}$$

from which we infer that

$$\frac{\alpha}{2}=\phi_b-\phi_P=\cos^{-1}\left[\frac{\cos\theta_b-\cos\theta\cos\theta_a}{\sin\theta\sin\theta_a}\right] \tag{4.4.11}$$

Following the same lines we can find $\beta/2$ as given by a similar equation: we must only exchange θ_a and θ_b in the above result

$$\frac{\beta}{2}=\cos^{-1}\left[\frac{\cos\theta_a-\cos\theta\cos\theta_b}{\sin\theta\sin\theta_b}\right] \tag{4.4.12}$$

The areas A_1 and A_2 can be obtained by means of a known theorem for spherical triangles, which states that

$$(\text{sum of internal angles})-\pi=\frac{area}{R^2} \tag{4.4.13}$$

where R is the radius of the spherical surface over which the triangle lays and in our case is equal to unity. For the area A_1 we deduce

$$\frac{\alpha}{2}+\xi-\frac{\pi}{2}=A_1 \tag{4.4.14}$$

where ξ is the angle between the lines QS and RS. In Fig.4.4 we show how this area arises from the intersection of the great circles inscribed over the spherical surface.

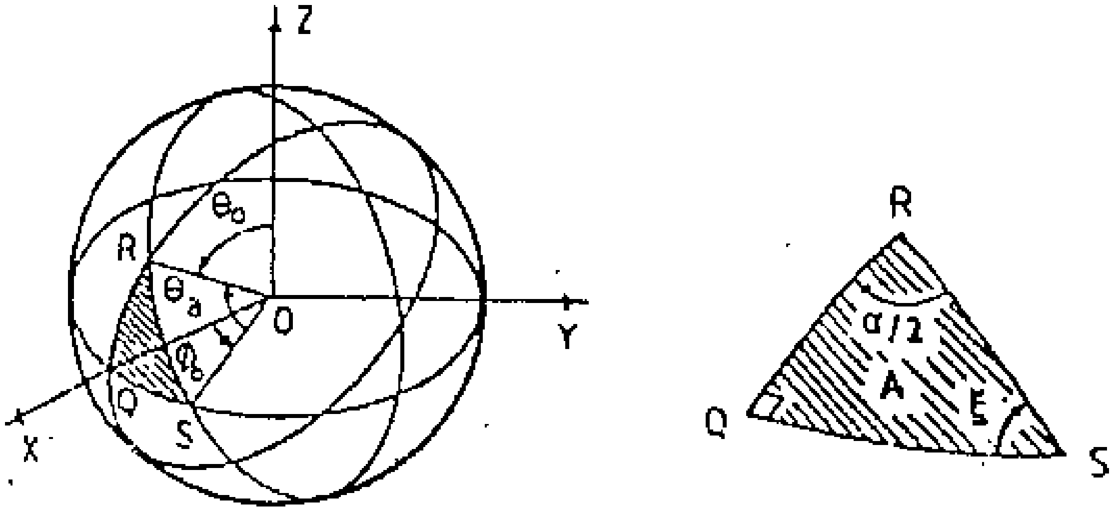

Fig.4.4: Three great circles over the spherical surface and a spherical triangle of and A limited by the segments of their intersections. With respect to a conveniently chosen coordinates-axis system, R lies on the XZ-plane and has polar coordinate θ_0, S lies on the XY-plane and has azimuthal coordinates ϕ_0. The angle between the lines joining R and S to the origin is θ_a. From this picture one deduces the internal angles $\frac{\alpha}{2}$ and ξ of the spherical triangle as functions of θ_0, ϕ_0 and θ_a.

Now the z-axis is chosen so that the line QS lies on a great circle in the XY-plane and the line RQ lies on a great circle in the plane XZ. The angle ξ will be given by the scalar product between a unitary vector perpendicular to the great circle which contains the lines RS and a unitary vector in the Z-direction. In terms of the auxiliary angles θ_0 and ϕ_0, we obtain

$$\xi = \cos^{-1}\left[\frac{\sin\theta_0 \sin\phi_0}{\sqrt{\cos^2\theta_0 + \sin^2\theta_0 \sin^2\phi_0}}\right] \tag{4.4.15}$$

Taking the scalar product of the same unit vector in the Y-direction, we find

$$\frac{\alpha}{2} = \cos^{-1}\left[\frac{\cos\theta_0 \cos\phi_0}{\sqrt{\cos^2\theta_0 + \sin^2\theta_0 \sin^2\phi_0}}\right] \tag{4.4.16}$$

The angle θ_a is also related with θ_0 and ϕ_0 by

$$\cos\theta_a = \sin\theta_0 \cos\phi_0 \tag{4.4.17}$$

Eliminating θ_0 and ϕ_0 from these relations and using Eqn. (4.4.11), we obtain

$$\frac{\pi}{2}-\xi=\cos^{-1}\left[\frac{\cos\theta_b-\cos\theta\cos\theta_a}{\sin\theta_a\sqrt{\cos^2\theta_a+\cos^2\theta_b-2\cos\theta\cos\theta_a\cos\theta_b}}\right] \tag{4.4.18}$$

Substituting Eqn. (4.2.11) and Eqn. (4.2.18) in Eqn. (4.2.14) we get

$$A_1=\cos^{-1}\left[\frac{\cos\theta_b-\cos\theta\cos\theta_a}{\sin\theta\sin\theta_a}\right]-\cos^{-1}\left[\frac{\cos\theta_b-\cos\theta\cos\theta_a}{\sin\theta_a\sqrt{\cos^2\theta_a+\cos^2\theta_b-2\cos\theta\cos\theta_a\cos\theta_b}}\right] \tag{4.4.19}$$

Following the same procedure we can find a similar equation for A_2

$$A_2=\cos^{-1}\left[\frac{\cos\theta_a-\cos\theta\cos\theta_b}{\sin\theta\sin\theta_b}\right]-\cos^{-1}\left[\frac{\cos\theta_a-\cos\theta\cos\theta_b}{\sin\theta_b\sqrt{\cos^2\theta_a+\cos^2\theta_b-2\cos\theta\cos\theta_b\cos\theta_a}}\right] \tag{4.4.20}$$

Gathering these results in Eqn. (4.4.9) we finally find that

$$\begin{aligned}\overline{\Omega}(\theta,\theta_a,\theta_b)=2\Bigg\{&\cos^{-1}\left[\frac{\cos\theta_b-\cos\theta\cos\theta_a}{\sin\theta_a\sqrt{\cos^2\theta_a+\cos^2\theta_b-2\cos\theta\cos\theta_a\cos\theta_b}}\right]\\&+\cos^{-1}\left[\frac{\cos\theta_a-\cos\theta\cos\theta_b}{\sin\theta_b\sqrt{\cos^2\theta_a+\cos^2\theta_b-2\cos\theta\cos\theta_b\cos\theta_a}}\right]\\&-\cos\theta_a\cos^{-1}\left[\frac{\cos\theta_b-\cos\theta\cos\theta_a}{\sin\theta\sin\theta_a}\right]\\&-\cos\theta_b\cos^{-1}\left[\frac{\cos\theta_a-\cos\theta\cos\theta_b}{\sin\theta\sin\theta_b}\right]\Bigg\}\end{aligned} \tag{4.4.21}$$

for $\quad |\theta_a-\theta_b|\le\theta\le\theta_a+\theta_b$

Thus using Eqn. (4.4.21) in Eqn. (4.4.6) we may easily obtain the Pauli blocking effect Ω_{Pauli}. Now this Ω_{Pauli} may be used in Eqn. (4.4.2), so that after using the cross-section σ_{NN}^{free} for free NN-scattering obtained from the Golden rule formula (section 4.3) ensures the derivation of the NN-cross-section in a nucleon medium.

4.5 Density dependence of in-medium NN cross sections:

The nucleon-nucleon cross section is a fundamental input in theoretical calculations of nucleus-nucleus collisions at intermediate and high energies ($\varepsilon / A \geq 100$ MeV). One expects to obtain information about the nuclear equation of state by studying global collective variables in such collisions [43]. In previous theoretical studies of heavy-ion collisions at intermediate energies ($\varepsilon / A \simeq 100$ MeV) the nucleon-nucleon cross-section was multiplied with a constant scaling factor to account for in-medium corrections [44, 45]. As pointed out in [46], this approach fails in low-density nuclear matter where the in-medium cross-section should approach its free-space value. A more realistic approach uses a Taylor expansion of the in-medium cross-section in the density variable. One obtains [47]

$$\sigma_{NN} = \sigma_{NN}^{free}(1+\alpha\,\overline{\rho}) \tag{4.5.1}$$

where $\overline{\rho} = \rho/\rho_0$, ρ_0 is the normal nuclear density and α is the logarithmic derivative of the in-medium cross section with respect to the density, taken at $\rho = 0$,

$$\alpha = \rho_0 \frac{\partial}{\partial \rho}(\ln \sigma_{NN})_{|\rho=0} \tag{4.5.2}$$

This parametrization is motivated by Brueckner G-matrix theory and is basically due to Pauli-blocking of the cross-section for collisions at intermediate energies [48]. Values of α between -0.4 and -0.2 yield the best agreement with involved G-matrix calculations using realistic nucleon-nucleon interactions [48].

In this section, we give a simple and transparent derivation of the lowest-order expansion of the in-medium nucleon-nucleon cross section in terms of the nucleon density. Here two approximations can be done: (a) on average, the symmetric situation in which $k_{F1} = k_{F2} \equiv k_F$, $q = k_0/2$, $p = k_0/2$ and $b = k_0/2$, is favoured; (b) the free nucleon-nucleon cross section can be taken outside of the integral in Eqn. (4.4.2). Both approximations are supported by the studies of [49]. The assumption (a) implies that $\Omega_c = \Omega_b = \overline{\Omega}$. So we obtain from Eqn. (4.4.6)

$$\begin{aligned}\Omega_{Pauli} &= 4\pi - 2\Omega_a \\ &= 4\pi - 4\pi(1-\cos\theta_a) \\ &= 4\pi\left(1-2\frac{k_F^2}{k_0^2}\right)\end{aligned} \tag{4.5.1}$$

Furthermore, assumption (b) implies that

$$\sigma_{NN}(k_0,k_F) = \sigma_{NN}^{free}(k_0)\int\frac{d^3k_1 d^3k_2}{(4\pi k_{F1}^3/3)(4\pi k_{F2}^3/3)}\frac{\Omega_{Pauli}}{4\pi}$$

$$= \sigma_{NN}^{free}(k_0)\frac{1}{(4\pi k_{F1}^3/3)(4\pi k_{F2}^3/3)}\int_0^{k_{F1}} d^3k_1 \int_0^{k_{F2}} d^3k_2 \frac{\Omega_{Pauli}}{4\pi}$$

6

$$= \sigma_{NN}^{free}(k_0)\frac{\Omega_{Pauli}}{4\pi} = \sigma_{NN}^{free}(k_0)\left(1-2\frac{k_F^2}{k_0^2}\right) \tag{4.5.2}$$

The above equation shows that the in-medium nucleon-nucleon cross section is about 1/2 of its free value for $k_0 = 2k_F$, i.e. for $\varepsilon / A \simeq 150$ MeV, in agreement with the numerical results of [49]. The connection with the nuclear densities is accomplished through the local density approximation, which relates the Fermi momenta to the local densities as

$$k_F^2 = \left[\frac{3}{2}\pi^2\rho(r)\right]^{2/3} + \frac{5}{2}\xi\left[(\nabla\rho)/\rho\right]^2 \tag{4.5.3}$$

where $\rho(r)$ is the sum of nucleon densities of each colliding nucleus at the position r. The second term is small and amounts to a surface correction, with ξ of the order of 0.1 [49]. Neglecting the second term of Eqn. (4.5.3) and inserting it in Eqn. (4.5.2), together with the relations $E = \hbar^2 k_0^2/2m_N$ and $\bar{\rho} = \rho/\rho_0$ gives us

$$\sigma_{NN}(E,\rho) = \sigma_{NN}^{free}(E)\left(1+\frac{-\hbar^2\left[\frac{3}{2}\pi^2\rho_0\right]^{2/3}}{Em_N}\bar{\rho}^{2/3}\right)$$

$$= \sigma_{NN}^{free}(E)\left(1+\alpha'\bar{\rho}^{2/3}\right) \quad \text{where} \quad \alpha' = -\frac{\hbar^2\left[\frac{3}{2}\pi^2\rho_0\right]^{2/3}}{Em_N} \tag{4.5.4}$$

Taking $\rho_0 = .18 fm^{-3}$ and the nucleon mass $m_N = 1.67265 \times 10^{-24} gm$ we obtain

$$\alpha' = -\frac{79.76}{E(MeV)} \tag{4.5.5}$$

where E is the energy per nucleon $\mathcal{E} / A$.

The above equation shows that the local density approximation leads to a density dependence proportional to $\bar{\rho}^{2/3}$. The Pauli principle yields a $1/E$ dependence on the bombarding energy. This behaviour arises from a larger phase space available for nucleon-nucleon scattering with increasing energy. The nucleon-nucleon cross section at $E \leq 300$ MeV decreases with E approximately as $1/E$. Thus we expect that, in nucleus-nucleus collisions, this energy dependence is flattened by the Pauli correction, i.e. the in medium nucleon-nucleon cross section is flatter as a function of E, for $E \leq 300$ MeV, than the free cross section. For higher values of E the Pauli blocking is less important and the free and in-medium nucleon-nucleon cross-sections are approximately equal. These conclusions are in agreement with the experimental data for nucleus-nucleus reaction cross-section [50] Here we have considered the energies up to 300 MeV. At energies above 300 MeV, inelastic channels enter into the picture. We note that, for $E = 150 - 300$ MeV, and $\rho \approx \rho_0$ Eqn. (4.5.5) yields a coefficient α' between -0.2 and -0.5. This is in excellent agreement with the findings based on the BUU (Boltzmann-Uehling-Uhlenbeck) [46] calculations, primarily intended to reproduce the experimental data on intermediate energy nucleus-nucleus collisions.

Conclusion

In chapter one, we have given a brief review of the meson theory, nuclear force and the properties of the nuclear matter structure.

In chapter two, we have derived the one-boson exchange Bonn potentials using the Feynman rules for the scattering of free nucleons for various boson fields such as scalar, psuedoscalar and vector fields.

In chapter three, we have first discussed the non-relativistic Brueckner G-matrix theory for nucleon-nucleon scattering in the nuclear matter, where the in-medium effect has been described by the Pauli project operator. For a relativistic extension of Brueckner theory we have considered the Thompson equation which is a 3-dimensional reduction of the 4-dimensional Bethe-Salpeter equation describing the free NN interaction. Then, in the framework of Dirac-Brueckner approach for the in-medium effect, we have derived the relativistic G-matrix equation, where the NN interaction has been described by the one-boson-exchange Bonn potentials and the solution of the Dirac's relativistic wave equation has been taken into account.

In Chapter four, we have discussed a method: the matrix inversion method to solve the G-matrix equation and hence to study the saturation properties of the nuclear matter as well as to calculate the in-medium cross-sections directly from the G-matrix. We have also discussed the in-medium NN cross-sections in an alternative way in terms of the free NN cross-sections obtained from the Golden Rule, where the in-medium corrections are obtained from the geometrical considerations of the Pauli blocking effect.

Finally, we have considered some approximations in this alternative approach. In the simplest case the lowest-order correction of the density dependence of the in-medium NN cross-sections imply an $1/E$ energy dependence of the density dependent term. This shows that for high energy values the Pauli-blocking i.e. the medium effect is less important and the free and in-medium NN cross-section becomes approximately equal.

To conclude, we may say that this work may be considered as a basis for studying the nuclear structure properties and for calculating the in-medium NN cross-sections in two alternative ways: One from the Dirac-Brueckner *G*-matrix directly which involves the different Bonn potentials for the NN interaction and the other from the free NN cross-section including the Pauli blocking for the in-medium effect, where all the necessary derivation and formulation have been done

So, in future, this work may be extended to a numerical work for computation and comparison of the in-medium NN cross-sections in two alternative ways. It may also be extended for calculation of the single particle energy as a function of density in the nuclear medium and hence to study the saturation properties of the nuclear matter.

References

[1] K. A. Brueckner, C. A. Levinson and H. M. Mahmoud, "Two-Body Forces and Nuclear Saturation. I. Central Forces", Phys. Rev. **95**, No.1, 217 (1954).

[2] H. A. Bethe, "Nuclear Many-Body Problem", Phys. Rev. **103**, 1353 (1956).

[3] M. I. Haftel and F. Tabakin, "Nuclear Saturation and the Smoothness of Nucleon-Nucleon Potentials", Nucl. Phys. **A158**, 1 (1970).

[4] B. D. Day, "Elements of the Brueckner-Goldstone Theory of Nuclear Matter", Rev. Mod. Phys. **39**, 719 (1967),

[5] B. D. Day, "Exact Treatment of the Coulomb Exchange Interaction in Heavy-Ion Collisions and its Effect on Elastic $^{16}O-^{16}O$ and $\alpha-^{18}O$ Scattering", Phys. Rev. **C24**, 1023 (1981).

[6] I. Bombaci and Lombardo, "Asymmetric Nuclear Matter Equation of State", Phys. Rev. C44, 1892 (1991).

[7] K. Holinde, "Two-Nucleon Forces and Nucleon Matter", Phys. Rep. **68**, 121 (1981).

[8] R. Machleidt, "The Meson Theory of Nuclear Forces and Nuclear Structure", Adv. Nucl. Phys. **19**, 189 (1989).

[9] B. ter Haar and R. Malfliet, "Equation of State of Dense Asymmetric Nuclear Matter", Phys. Rev. Lett. **59**, No.15, 1652 (1987).

[10] L. D. Miller and A. E. S. Green, "Relativistic Self-Consistent Meson Field Theory of Spherical Nuclei", Phys. Rev. **C 5**, No.1, 241 (1972).

[11] L. G. Arnold, B. C. Clark and R. L. Mercer, "Relativistic Optical Model Analysis of Medium Energy P–^{4}He Elastic Scattering Experiments", Phys. Rev. C **19**, No. 3, 917 (1979)

[12] M. R. Ansatasio, L. S. Celenza, W. S. Pong and C. M. Shakin, "Relativistic Nuclear Structure Physics", Phys. Rep. **100**, No. 6, 327 (1983).

[13] G. F. Bertsch and S. Das Gupta, "A Guide to Microscopic Models for Intermediate Energy Heavy Ion Collisions", Phys. Rep. **160**, No.4, 190 (1988).

[14] G. E. Brown, V. Koch and M. Rho, "The Pion at Finite Temperature and Density", Nucl. Phys. **A535**, 701 (1991).

[15] E. E. Salpeter and H. A. Bethe, "A Relativistic Equation for Bound-State Problems", Phys. Rev. **84**, No. 6, 1232 (1951).

[16] M. Lacombe, B. Loiseau, J. M. Richard R. Vinh Mau, J. Cote, P. Pires and R. de Tourreil, "Parameterization of the Paris N-N Potential", Phys Rev. **C21**, 861 (1980).

[17] M. H. Partovi and E. L. Lomon, "Field-Theoretical Nucleon-Nucleon Potential", Phys. Rev. **D2**, 1999 (1970).

[18] R. Blankenbecler and R. Sugar, "Linear Integral Equations for Relativistic Multi-channel Scattering", Phys. Rev. **142**, No. 4, 1051 (1966).

[19] R Machleidt, K. Holinde and C. Elster, "The Bonn Meson-Exchange Model for the Nucleon-Nucleon Interaction", Phys. Rep. **149**, 1 (1987).

[20] H. P. Stapp, T. J. Ypsilantis and N. Metropolis, "Phase-Shift Analysis of 310 MeV Proton Proton Scattering Experiments", Phys. Rev. **105**, 302 (1957).

[21] J. L, Gammel and R. M. Thaler, "Spin-Orbit Coupling in the Proton-Proton Interaction", Phys. Rev. **107**, No.1, 291, (1957).

[22]. J. L, Gammel and R. M. Thaler, "Spin-Orbit Coupling in the Neutron-Proton Interaction", Phys. Rev. **107**, No.5, 1337 (1957).

[23] Atomic Data and Nuclear Data Tables 17, No. 5–6, p 67-91, (1976).

[24] X. Campi and D. W. L. Sprung, "Spherical Nuclei in the Local Density Approximation", Nucl. Phys. **194**, 401 (1972).

[25] G. Fai and J. Nemeth, "Density Dependent Effective Interactions in Finite Nuclei (II)", Nucl. Phys. **A208**, 463 (1973).

[26] C. J. Horowitz and B. D. Serot, "Self-Consistent Hartree Description of Finite Nuclei in a Relativistic Quantum Field Theory", Nucl. Phys. **A368**, 503 (1981);

[27] M. Waroquier, K. Heyde and G. Wenes, "An effective Skyrme-Type Interaction for Nuclear Structure Calculations", Nucl. Phys. **A404**, 269 (1983);

[28] A. K. Dutta, J. P. Arcoragi, J. M. Pearson, R. Behrman and F. Tondeur, "Thomas-Fermi Approach to Nuclear Mass Formula (1). Spherical Nuclei", Nucl. Phys. **A458**, 77 (1986).

[29] D. Griffiths, "Introduction to Elementary Particles", p189, John Wiley & Sons.INC.

[30] S. Weinberg, "Dynamical Approach to Current Algebra", Phys. Rev. Lett. **18**, No.5, 188 (1967).

[31] G. E. Brown, "Mesons in Nuclei", Vol.-I, p.330, North Holland, Amsterdam (1979).

[32] H. A. Bethe, B. H. Brandow and A. G. Petshek, "Reference Spectrum Method for Nuclear Matter", Phys. Rev., **129**, 225 (1963)

[33] R. Rajaraman and H. A. Bethe, "Three-Body Problem in Nuclear Matter", Rev. Mod. Phys. **39**, 745 (1967).

[34] G. Q. Li, R. Machleidt and R. Brockmann, "Properties of Dense Nuclear and Neutron Matter with Relativistic Nucleon-Nucleon Interactions", Phys. Rev. **C 45**, No. 6, 2782 (1992).

[35] R. H. Thompson, "Three-Dimensional Bethe-Salpeter Equation Applied to the Nucleon-Nucleon Interaction", Phys. Rev. **D1**, No. 1, 110 (1970).

[36] M. R. Anastasio, L. S. Celenza and C. M. Shakin, "Relativistic Effects in the Bethe-Brueckner Thoery of Nuclear Matter", Phys. Rev. **C23**, No. 5, 2273 (1981).

[37] C. J. Horowitz and B. D. Serot, "Two-Nucleon Correlations in a Relativistic Theory of Nuclear Matter", Phys. Lett. **137B**, No. 5–6, 287 (1984).

[38] R. Brockmann and R. Machleidt, "Nuclear Saturation in a Relativistic Brueckner-Hartree-Fock Approach", Phys. Lett. **149B**, No. 4–5, 283 (1984).

[39] B. ter Haar and R. Malfliet, "Pion Production, Pion Absorbption and Nucleon Properties in a Dense Nuclear Matter: Relativistic Dirac-Brueckner Approach at Intermediate and High Energies", Phys. Rev. **C36**, No. 4, 1611 (1987).

[40] B. ter Haar and R. Malfliet, "Nucleons, Mesons and Deltas in Nuclear Matter: A Relativistic Dirac-Brueckner Approach", Phys. Rep. **149**, No. 4, 207 (1987).

[41] N. J. Digiacomo, R. M. Devries and J. C. Peng, "Microscopic Description of Nucleon-Nucleus Total Reaction Cross-Sections", Phys. Rev. Lett. **45**, 527 (1980).

[42]. C. A. Bertulani, "Heavy Ion Reaction Cross-Sections", Braz. J. Phys. **16**, No.3, 380 (1986).

[43] H. H. Gutbrot, A. M. Poskanger and H. G. Ritter, "Plastic Ball Experiments", Rep. Prog. Phys. **52**, 1267 (1989).

[44]. G. F. Bertsch, W. G. Lynch and M. B Tsang, "Transverse Momentum Distributions in Intermediate-Energy Heavy-Ion Collisions", Phys. Lett. **B 189**, No.4, 384 (1987).

[45] W. Bauer, "Nuclear Stopping at Intermediate Beam Energies", Phys. Rev. Lett. **61**, No.22, 2534 (1988).

[46]. G. D. Westfall et al., "Mass Dependence of the Disappearance of Flow in Nuclear Collisions", Phys. Rev. Lett. **71**, No.13, 1986 (1993).

[47]. D. Klakow, G. Welke and W. Bauer, "Nuclear Flow Excitation Function", Phys. Rev. C **48**, No.4, 1982 (1993).

[48]. T. Alm, G. Röpke, W. Bauer, F. Daffin and M. Schmidt, "The In-Medium Nucleon-Nucleon Cross-Section and BUU Simulations of Heavy-Ion Reactions", Nucl. Phys. **A587**, 815 (1995).

[49]. M. S. Hussein, R. A. Rego and C. A. Bertulani, "Microscopic Theory of the Total Reaction Cross-Section and Application to Stable and Exotic Nuclei", Phys. Rep. **201**, No. 5, 279 (1991).

[50]. S. Kox, A Gamp, C. Perrin, J. Arvieux, R. Bertholet, J. F. Bruandet, M. Buenerd, Y. El Masri, N. Longequene and F. Merchez, "Transparency Effects in Heavy-Ion Collisions Over the Energy Range 100–300 MeV/Nucleon", Phys. Lett. **B159**, No.1, 15 (1985).